คุณสมบัติแฟรกทัลของเสี้ยนใยกระดูกเพื่อประเมินเสถียรภาพของรากฟันเทียม

นางสาวนภัสสร กังวานสุรกิจ

วิทยานิพนธ์นี้เป็นส่วนหนึ่งของการศึกษาตามหลักสูตรปริญญาวิทยาศาสตรมหาบัณฑิต
สาขาวิชารังสีวิทยาช่องปากและแม็กซิลโลเฟเชียล ภาควิชารังสีวิทยา
คณะทันตแพทยศาสตร์ จุฬาลงกรณ์มหาวิทยาลัย
ปีการศึกษา 2559

FRACTAL PROPERTIES OF BONE TRABECULAE FOR IMPLANT STABILITY EVALUATION

Miss Napassorn Kangvansurakit

A Thesis Submitted in Partial Fulfillment of the Requirements

for the Degree of Master of Science Program in Oral and Maxillofacial Radiology

Department of Radiology

Faculty of Dentistry

Chulalongkorn University

Academic Year 2016

Thesis Title	FRACTAL PROPERTIES OF BONE TRABECULAE FOR IMPLANT STABILITY EVALUATION
By	Miss Napassorn Kangvansurakit
Field of Study	Oral and Maxillofacial Radiology
Thesis Advisor	Associate Professor Patita Bhuridej, Ph.D.

Accepted by the Faculty of Dentistry, Chulalongkorn University in Partial Fulfillment of the Requirements for the Master's Degree

.....Dean of the Faculty of Dentistry

(Assistant Professor Suchit Poolthong, Ph.D.)

THESIS COMMITTEE

.....Chairman

(Professor (Clinical) Wichitsak Cholitgul)

.....Thesis Advisor

(Associate Professor Patita Bhuridej, Ph.D.)

.....Examiner

(Vannaporn Chuenchompoonut, Ph.D.)

.....External Examiner

(Associate Professor Sangsom Prapayasatok)

นภัสสร กังวานสุรกิจ : คุณสมบัติแฟรกทัลของเสี้ยนใยกระดูกเพื่อประเมินเสถียรภาพของรากฟันเทียม (FRACTAL PROPERTIES OF BONE TRABECULAE FOR IMPLANT STABILITY EVALUATION) อ.ที่ปรึกษาวิทยานิพนธ์หลัก: รศ. ทญ. ดร.ภาฑิตา ภูริเดช, 90 หน้า.

วัตถุประสงค์: งานวิจัยนี้มุ่งศึกษาความสัมพันธ์ระหว่างค่ามิติแฟรกทัลของเสี้ยนใยกระดูก (FD) และค่าเสถียรภาพของรากฟันเทียมแบบควอเทียน (ISQ) และค่าแรงการใส่รากเทียม (IT)

วิธีการวิจัย: ผู้ป่วยซึ่งได้รับการฝังรากฟันเทียม ณ คณะทันตแพทยศาสตร์ จุฬาลงกรณ์มหาวิทยาลัย ในระหว่าง พ.ศ. 2554 – 2560 ได้รับการคัดกรองตามเกณฑ์การเข้าร่วมการวิจัย ซึ่งได้แก่ การปรากฏค่า ISQ และ IT ในแฟ้มประวัติ และการปราศจากโรคทางระบบที่กระทบต่อคุณภาพของกระดูก ข้อมูลพื้นฐานของผู้ป่วยและรายละเอียดการฝังรากฟันเทียมได้รับการคัดแยกและเก็บ ค่า FD ได้รับการคำนวณจากภาพรังสีตัดขวางซึ่งถ่ายภายใน 6 เดือนก่อนการฝังรากเทียม โดยทำการเก็บข้อมูลค่าปัจจัยที่เกี่ยวข้องในการถ่ายภาพร่วมด้วย การทดสอบความแตกต่างของค่ากลางของสองประชากรไม่อิสระระหว่างพื้นที่การคำนวนค่า FD ที่เน้นความกว้างและความยาวของกระดูกใช้เพื่อเลือกพื้นที่ในการคำนวนค่า FD การวิเคราะห์ข้อมูลตัวแปรเดียวใช้เพื่อหาปัจจัยที่มีผลต่อ ISQ และ IT จากนั้นปัจจัยที่พบความสัมพันธ์อย่างมีนัยสำคัญจะได้รับการพิจารณาอีกครั้งด้วยการวิเคราะห์สมการถดถอยพหุคูณเพื่อทดสอบความสัมพันธ์ระหว่างค่า FD และค่า ISQ และ IT

ผลการวิจัย: ค่า FD จากพื้นที่การคำนวนทั้ง 2 แบบไม่แตกต่างอย่างมีนัยสำคัญ (p=0.779) เส้นผ่านศูนย์กลางของรากฟันเทียมและขากรรไกรที่ได้รับการรักษามีผลต่อค่า ISQ อย่างมีนัยสำคัญทางสถิติ (p <0.001) ค่า FD ไม่มีความสัมพันธ์อย่างมีนัยสำคัญกับค่า ISQ ในขณะที่ปัจจัยอื่นๆ ไม่มีผลต่อค่า IT และค่า FD มีความสัมพันธ์อย่างมีนัยสำคัญทางสถิติกับค่า IT ในขากรรไกรล่าง โดยมีสมการความสัมพันธ์คือ IT = 92.168 – 71.112(FD) (R^2 = 0.145, p = 0.026)

สรุปผลการวิจัย: ค่า FD ของเสี้ยนใยกระดูกจากภาพรังสีก่อนการฝังรากฟันเทียมมีความสัมพันธ์เชิงเส้นอย่างมีนัยสำคัญทางสถิติกับค่า IT ในขากรรไกรล่าง แต่ไม่มีความสัมพันธ์อย่างมีนัยสำคัญระหว่างค่า FD กับค่า ISQ ภายใต้เงื่อนไขของการศึกษานี้ โดยพบว่าค่า ISQ ได้รับผลกระทบจากขนาดเส้นผ่านศูนย์กลางของรากฟันเทียมและขากรรไกรที่ทำการฝังรากฟันเทียม

ภาควิชา รังสีวิทยา ลายมือชื่อนิสิต .....

สาขาวิชา รังสีวิทยาช่องปากและแม็กซิลโลเฟเชียล ลายมือชื่อ อ.ที่ปรึกษาหลัก .....

ปีการศึกษา 2559

5875838132 : MAJOR ORAL AND MAXILLOFACIAL RADIOLOGY
KEYWORDS: CBCT / FRACTAL DIMENSION / IMPLANT STABILITY QUOTIENT / INSERTION TORQUE

NAPASSORN KANGVANSURAKIT: FRACTAL PROPERTIES OF BONE TRABECULAE FOR IMPLANT STABILITY EVALUATION. ADVISOR: ASSOC. PROF. PATITA BHURIDEJ, Ph.D., 90 pp.

Objectives: This investigation aimed to explore the correlation between fractal dimension (FD) and two primary implant stability parameters: Implant stability quotient (ISQ) and Insertion torque (IT).

Materials and methods: Patients, receiving implant placement at Faculty of Dentistry, Chulalongkorn University between 2011 and 2017, were screened according to study criteria. Demographic data of the patient and details of implant treatment were recorded. CBCT data acquired 6 months prior to implantation was used, while imaging related variables were documented. Paired t-test was applied between FD derived from areas emphasizing height and width. All possible affecting factors to ISQ and IT, including FD, were analyzed using univariate analysis. Subsequently, all factors with significant correlation were re-analyzed and adjusted with multiple linear regression.

Results: There was no difference between FD values from the 2 areas. ($p=0.779$) ISQ values were significantly affected by implant diameter and jaw bones. ($p <0.001$) No significant correlation was found between ISQ and FD. No confounding factor to IT was found. Significant correlation between IT and FD was revealed only in the mandible with a model: $IT = 92.168 – 71.112(FD)$. ($R^2 = 0.145$, $p = 0.026$)

Conclusion: A significant correlation was shown between FD and IT in mandibular samples. No correlation between FD and ISQ was found under this study condition. Implant diameter and jaw type for implantation were found to influence ISQ value.

Department: Radiology Student's Signature ----------
Field of Study: Oral and Maxillofacial Radiology Advisor's Signature ----------
Academic Year: 2016

ACKNOWLEDGEMENTS

The author would like to acknowledge with deep appreciation and gratitude for the help and support from all people involved in completing this thesis. First of all, I would like to thank Associate Professor Patita Bhuridej, my thesis advisor, for her advices and dedication. Secondly, I would like to thank Dr. Onanong Silkosessak for giving me the opportunity to explore this subject with her dedicated supports, kind encouragement and suggestions throughout the work. Third, I express my gratitude to the thesis committee for their helpful guidance. Moreover, I would like to acknowledge Department of Radiology, Faculty of Dentistry, Chulalongkorn University for their supports. Last but not least, I would like to give my special recognitions to my family and friends for the warm supports and understandings throughout every process of research progression.

CONTENTS

Page

THAI ABSTRACT iv

ENGLISH ABSTRACT v

ACKNOWLEDGEMENTS vi

CONTENTS vii

LIST OF TABLES x

LIST OF FIGURES xii

LIST OF ABBREVIATIONS xv

CHAPTER I INTRODUCTION 16

Background and Rationale 16

Research Questions 22

Objectives 22

Research Hypotheses 22

Expected Benefits and Applications 23

Research Design 23

Conceptual Framework 23

Keywords 23

CHAPTER II LITERATURE REVIEW 24

Implant Stability 24

Resonance Frequency Analysis 25

Factors Influencing Resonance Frequency Analysis 28

1) Implant design 28

2) Anatomical location 29

Page

3) Bone quality 29

4) Peri-implant condition 31

5) Orientation of transducer 31

Insertion Torque 32

Factors Influencing Insertion Torque 33

1) Bone density 33

2) Drilling dimension 34

4) Anatomical location 35

Fractal Property and Fractal Analysis 35

1) Simplified spatial methods 37

Morphological image processing 37

Erosion and its variants 38

Dilation and its variant 39

Skeletonization 41

1.1) Caliper method 42

1.2) Tile counting method 42

1.3) Extended counting method 43

1.4) Pixel dilation method 44

2) General spatial methods 44

2.1) Box counting method 45

2.2) Differential box counting method 45

2.3) Triangular prism method 46

Page

2.4) Intensity variance method 47
2.5) Hurst method 47
2.6) Variation method 48
2.7) Blanket method 48
3) Spectral methods 48
Fractal Bone Analysis 48
Factors Influencing Fractal Dimension Value from Radiographs 50
1) X-ray parameters 50
2) Region of interest (ROI) selection 51
3) Anatomical location 51
4) Imaging modalities 52
5) Algorithms used to calculate the fractal dimension 53
6) Image resolution 53
CHAPTER III RESEARCH METHODOLOGY 56
Materials and Methods 56
Statistical Analysis 57
CHAPTER IV RESULTS 59
Part I Comparison between HROI and WROI 59
Part II Regarding ISQ 59
Part III Regarding IT 67
CHAPTER V DISCUSSION AND CONCLUSION 73
Discussion 73

Page

Conclusions 81

REFERENCES 82

VITA 90

LIST OF TABLES

Page

Table 1. Interpretation of periotest reading between -8 to +50 20

Table 2. Misch bone density classification scheme 34

Table 3. Distribution of subjects for each implant parameter regarding ISQ affecting factors 60

Table 4. Univariate analysis results for each studied factors with possible influences on ISQ 61

Table 5. Distribution of maxillary subjects for each implant data and CBCT parameter in regarding to correlation between FD and ISQ 62

Table 6. Distribution of mandibular subjects for each implant data and CBCT parameter in regarding to correlation between FD and ISQ 63

Table 7. Univariate analysis results for correlation between ISQ and FD 64

Table 8. Distribution of subjects for multiple linear regression regarding ISQ affecting factors 65

Table 9. Multiple linear regression analysis of all factors affecting ISQ 66

Table 10. Distribution of subjects for each implant parameter regarding IT affecting factors 67

Table 11. Univariate analysis results for each studied factors with possible influences on IT 68

Table 12. Distribution of maxillary subjects for each implant data and CBCT parameter in regarding to correlation between FD and IT 69

Table 13. Distribution of mandibular subjects for each implant data and CBCT parameter in regarding to correlation between FD and IT 70

Table 14. Univariate analysis results for correlation between IT and FD 71

Table 15. Multiple linear regression analysis of all factors affecting correlation between IT and FD in mandibular group 72

LIST OF FIGURES

Page

Figure 1. Percussion or tapping test: clinical examination..... 17

Figure 2. Cutting torque resistance analysis..... 18

Figure 3. Insertion and reverse torque test:..... 19

Figure 4. Periotest (A) and Periotest M (B) : instruments..... 20

Figure 5. Resonance frequency analysis (RFA): system 21

Figure 6. Resonance frequency analysis (RFA): component..... 26

Figure 7. Mandibular cortical index 30

Figure 8. Grading for bone quality assessment. 30

Figure 9. Insertion torque measurement..... 32

Figure 10. Fractal object “Sierpinski sieve” 35

Figure 11. Fractal object “Koch snowflake, Koch curve or Koch island or Koch star” 36

Figure 12. Examples of fitting and hitting of the structuring element..... 37

Figure 13. Erosion process..... 38

Figure 14. Comparison between erosion and its variants..... 39

Figure 15. Dilation process. 40

Figure 16. Comparison between the effect of dilation and thickening..... 40

Figure 17. Effect of opening and closing process. 41

Figure 18. The effect of skeletonization 41

Figure 19. Caliper method 42

Figure 20. Demonstrate the Tile counting method and the Modified tile counting method..... 43

Figure 21. Tile counting method and Extended counting method..... 43

Figure 22. Determining the FD of the cross-sectional infarct scar edge..... 44

Figure 23. Example of an image intensity surface. 45

Figure 24. Differential box counting method. 46

Figure 25. Triangular prism method for calculating fractal dimension. 47

Figure 26. Intensity variance methods of 5 datasets of known theoretical fractal dimensions..... 47

Figure 27. shows the morphological binary image processing prior to FD calculation..... 57

Figure 28. Scatter plot between ISQ and FD 64

Figure 29. Scattered plot between IT and FD 71

Figure 30. Difference in trabecular pattern between maxillary and mandibular sample 79

LIST OF ABBREVIATIONS

BIC	=	Bone-implant contact
CBCT	=	Cone beam computed tomography
CNR	=	Contrast-to-noise ratio
D_h	=	Hausdorff- Besicovitch dimension
DICOM	=	Digital imaging and communications in medicine
D_T	=	Topological dimension
FA	=	Fractal analysis
FD	=	Fractal dimension
FOV	=	Field of view
ISQ	=	Insertion stability quotient
IT	=	Insertion torque
MCI	=	Mandibular cortical index
PVE	=	Partial volume effect
RFA	=	Resonance frequency analysis
ROI	=	Region of interest
TIFF	=	Tagged image file format

CHAPTER I
INTRODUCTION

Background and Rationale

Dental implant is now widely used for tooth substitution of partial or full edentulous patients. As a fixture integrates with bone recipient site, it provides support without the needs for neighboring teeth and reduces further alveolar resorption. Major advancements toward esthetic and more simplified methods are proposed. For example, immediate implant placement allows better preservation of bone and nicer soft tissue contour. [1] Moreover, immediate loading allows early function of the prosthesis. However, implant placement is an invasive multi-steps surgical procedure, demanding both time and financial expense with risks from post-operative complications and failures.

According to position statement of American Academy of Oral and Maxillofacial Radiology, dental radiographs are recommended in various steps of implant placement, including initial assessment of the overall dentition, pre-operative site-specific evaluation for implant planning and periodic post-operative implant monitoring. The need for cross-sectional images for specific site examination was re-emphasized with cone beam computed tomography as a method of choice. [2] Therefore, it is at best to maximize the diagnostic information, obtained from these radiographs, for the benefit of implant planning and prognostic prediction.

Implant stability is one of the key factors for the success of implant-supported restorations. [3] It is defined as clinical immobility of an implant or the ability to support axial, lateral and rotational loads; in other words, the suggested definition of osseointegration. [4, 5] As implant instability might lead to failures due to fibrous encapsulation [6, 7], this parameter plays major role in assessing treatment outcomes and long-term prognosis, as well as dictating time of loading, unloading or removing implant components. [3, 8-10]

Several techniques have been proposed in order to evaluate implant stability with different pros and cons. [9, 11, 12] For instance, **clinical perception test**, using blunt ended instruments to check for implant mobility, is simple and easy but considered as unpredictable and non-objective techniques. Clinical perception test, using **implant cutting resistance or seating torque test** is also possible during implant insertion, but it could provide false sense of stability with taper-shaped implants. [13] Additionally, only subjective evaluation could be obtained through these procedures.

Percussion test, via tapping handle of mouth-mirror against implant to produce ringing sound indicating good stability, is at best produce poor qualitative information. (Figure 1)

Figure 1. Percussion or tapping test: clinical examination

(Garry, B. Basel Dentist's blog[Online]. 2015. Available from : https://vimeo.com/111399434[2017,July 18])

Cutting torque resistance analysis (Figure 2) measures energy needed for electric handpiece to cut-off a volume of bone, which can be correlated to bone density. However, this technique can be done only during the stage I implant surgery.

Figure 2. Cutting torque resistance analysis.

(Koh, J. W., Yang, J. H., Han, J. S., Lee, J. B., and Kim, S. H. Biomechanical evaluation of dental implants with different surfaces: Removal torque and resonance frequency analysis in rabbits. J Adv Prosthodont 1 (July 2009): 107-112.)

Insertion torque (IT) is a mechanical parameter, measured only at the time of implant placement. It may be used as a stability measurement but it may also act as a factor, affecting implant stability. However, it cannot evaluate stability by new bone formation or remodeling around implant; therefore no longitudinal data can be collected.

Reverse or unscrewing torque test is recommended to be more than 20 Ncm during abutment connection; however, no lower threshold can be stated due to variations among patients. Additionally, this method does not provide information on lateral stability, while fracture of osseointegrated interface might be encountered from applied torque. Despite the fact that Ivanoff and colleagues [14] reported a possibility of re-integration if the implant was allowed to heal for an additional period of time, this technique was disregarded. [11] (Figure 3)

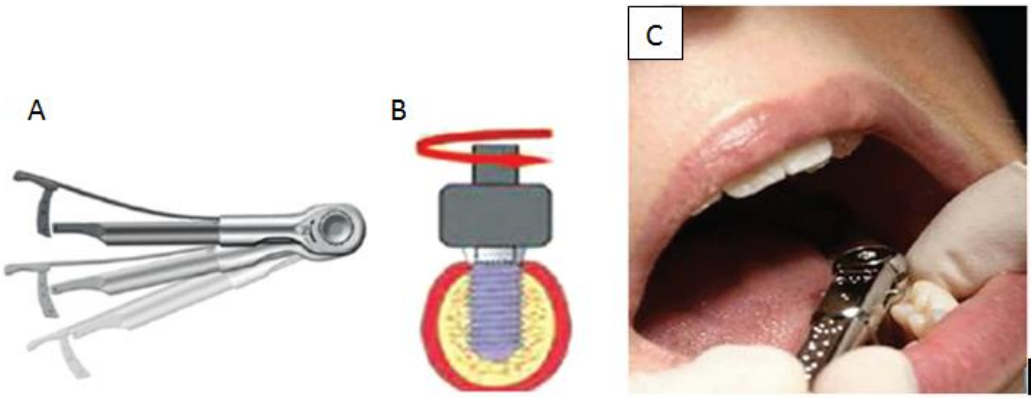

Figure 3. Insertion and reverse torque test:

A: Instrument B: Type of test (rotational torque) C: Clinical examination

(Swami, V., Vijayaraghavan, V., and Swami, V. Current trends to measure implant stability. J Indian Prosthodont Soc 16 (2016): 124-130

Mistry, G., Shetty, O., Shetty, S., and Singh, R. D. Measuring implant stability: A review of different methods. J Dent Impl 4 (2014): 165-169.)

Radiographic examinations are widely used to assess both quantity and quality of the jaw bones. [15] However, conventional radiographs do not provide information on facial bone level, whose loss precedes mesio-distal bone. [16]

Periotest (Figure 4) uses electrical device that measured the damping characteristic by percussing implant or implant assembly for totally 16 times in approximate 4 seconds and gives interpretative reading between -8 (low mobility) to +50 (high mobility) as shown in table 1. It can be applied at surgical stage I or post-operative visits. The drawbacks for this method are no absolute acceptable value available [17], no information regarding peri-implant bone level (only attribute to adjacent bone quality), and no diagnosis for implants with active integration process or borderline case, as successfully integrated implants have produced a wide reading range. In addition, it is easier to measure anterior implants but not posterior ones, in order to place the instrument perpendicularly to the axis of implant. Finally, this method is considered with poor sensitivity and is subjected to many variables. As a result, its reliability is questionable.

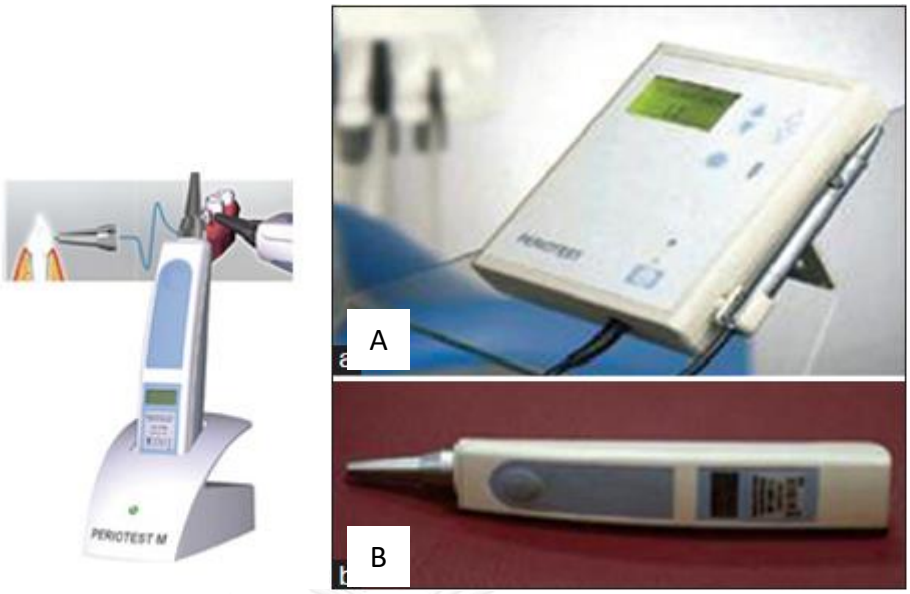

Figure 4. Periotest (A) and Periotest M (B) : instruments

(Periotester[Online]. Innovation service gestaltung DENTAL Gmbh, Available from: http://www.isg-gmbh.at/index.php?bid=245[2017,July 18]

Swami, V., Vijayaraghavan, V., and Swami, V. Current trends to measure implant stability. J Indian Prosthodont Soc 16 (2016): 124-130)

Reading	Interpretation
-8 to 0	Osseo integration is good, loading of implant can be done
+1 to 9	Examination is required, loading is not possible in many cases
+10 to +50	Osseo integration is not completed, implant cannot be loaded

Table 1. Interpretation of periotest reading between -8 to +50

Resonance frequency analysis (RFA) provides measurement values at any given times using structural and vibration principle with resonance frequency analyzer and transducer. (Figure 5)

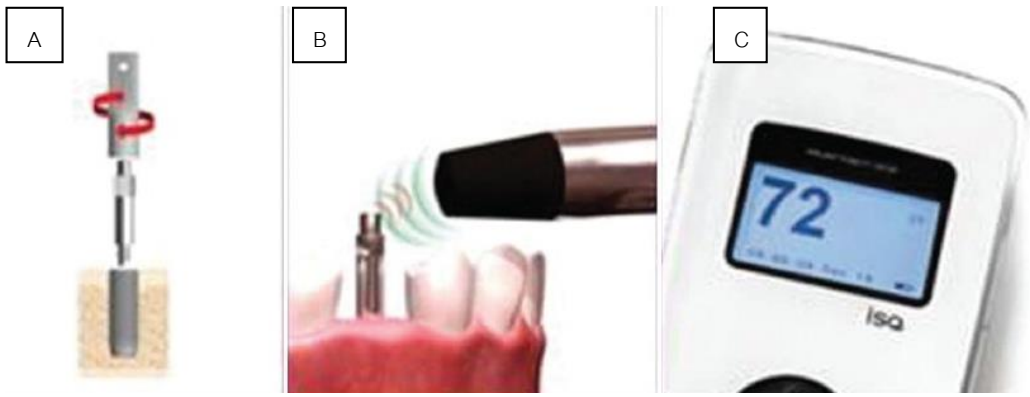

Figure 5. Resonance frequency analysis (RFA): system

A: Magnetic peg (smart peg^{TM}) B-C: Osstell ISQ^{TM}

(Swami, V., Vijayaraghavan, V., and Swami, V. Current trends to measure implant stability. J Indian Prosthodont Soc 16 (2016): 124-130)

RFA and IT, most commonly used clinical methods, which are currently applied in some cases at the Faculty of Dentistry, Chulalongkorn University, can provide non-invasive measurement for implant stability and bone osseointegration at implant placement and post-implant placement stages. [5, 10] RFA is based on structural and vibration principle, using resonance frequency analyzer and transducer. [3] For IT, a force needed to place the implant through pre-osteotomy site, is measured and inferred to bone density and hardness. [18] However, RFA requires specific instrument. The availability of RFA machine is limited and its application requires increased chair-time. For IT measurement, most implant systems do not provide electronic torque measuring device. Thus, the measurement relies on a torque gauge with unequal scaled markings or on the surgeon's experience. [18] Furthermore, both methods cannot give any pre-surgical diagnostic information, required for treatment planning and prognostic evaluation. It would be nice to have a procedure that can give information regarding implant stability using existing instrument or materials, or a procedure that can predict the treatment outcome in advance (pre-operatively) with less chair-time.

Advanced radiographic analysis of bone trabeculation in conventional or cone beam computed tomography (CBCT) might be useful in predicting implant stability outcome [5], as dental radiography already is a part of routine procedures in implant planning and post-operative evaluation, which provides both quantitative details of bone

dimension and qualitative information of bone density and microarchitecture, the two major influences on implant stability. A quantitative analysis of bone architectural quality can be achieve through fractal dimension analysis (FA), which is a non-invasive method to measure degree of bone complexity and might be considered as potential parameter to predict implant stability. [5] More studies are needed to test this possible association between bone fractal dimension (FD) and other implant stability parameters.

Research Questions

1) Is there any effect from non-standardized regions of interest (ROI) on radiographic bone fractal dimension? (height or width base area of ROI)
2) Is there any effect from studied factors (ie. sex, age, anatomical site, implant geometry--shape and thread designs, implant size--diameter and length) on insertion torque and implant stability quotient?
3) Is there any association between pre-surgical peri-implant bone fractal dimension to insertion torque and/or implant stability quotient?

Objectives

1) To investigate effect of difference in pixel area of ROIs on radiographic bone fractal dimension.
2) To identify significant affecting factors on insertion torque and implant stability quotient value, among studied factors.
3) To study an association between pre-surgical peri-implant bone fractal dimension to insertion torque and/or implant stability quotient.

Research Hypotheses

1) There is no significant difference among fractal dimension from studied factors. (height or width base area and pixel area of ROI)

2) There is no significant difference among insertion torque and implant stability quotient from studied factors. (sex, age, anatomical site, Implant geometry -- shape and thread design, implant size –diameter and length)

3) There are associations between pre-surgical peri-implant bone fractal dimension and insertion torque and/or implant stability quotient.

Expected Benefits and Applications

1) To know the factors influencing insertion torque and implant stability quotient.

2) To know the relationship between fractal dimension to insertion torque and/or implant stability quotient for primary stability.

Research Design

Retrospective analytical research

Conceptual Framework

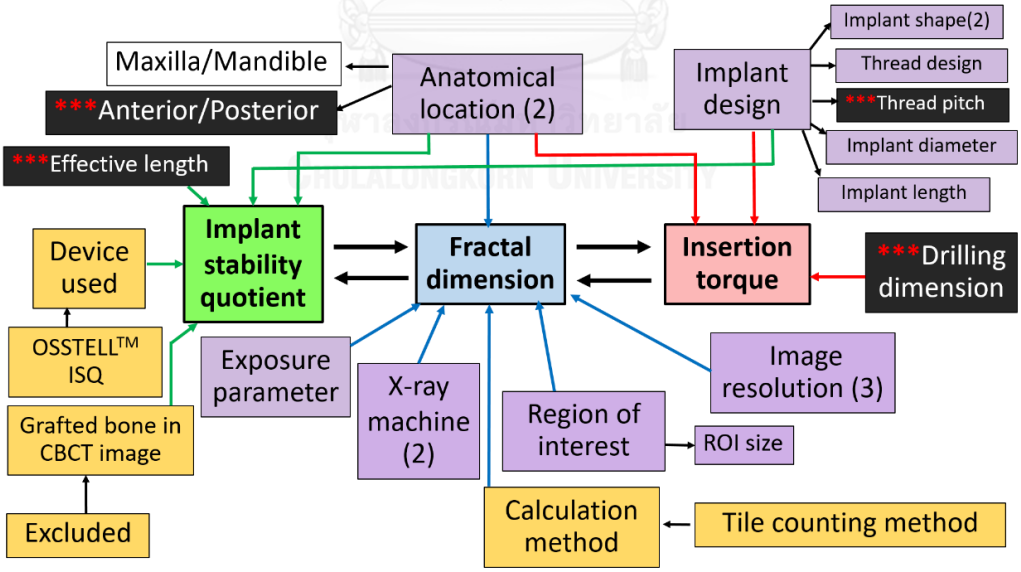

Keywords

CBCT, fractal dimension, implant stability quotient, insertion torque

CHAPTER II
LITERATURE REVIEW

Implant Stability

Implant stability can be divided into 2 phrases; primary and secondary stability. **Primary stability** depends mostly on immediate mechanical engagement between implant and surrounding bone during implantation. [10] Various factors can affect degree of primary stability, including quantity and quality of bone, implant geometry (length, diameter, shape and threads), surgical technique, occlusal load and occlusal restoration. [4] **Secondary stability**, beginning approximately at 4 weeks after implantation, is achieved through osseointegration, a biological healing process via bone regeneration and remodeling where implant surface is in direct structural and functional connection with newly formed bone without any fibrous or connective tissue separation. [3, 19] Osseointegration is believed to be completed within 8 weeks of placement, under normal conditions. [20] Primary stability is a prerequisite for a following successful secondary stability since implant micromotion at bone-implant interface between 50-150 μm can cause negative outcome in osseointegration with fibrous tissue formation. [3, 5, 21] Hence, secondary stability depends on patient-dependent wound healing ability. [10] It also affected by bone trabecular pattern, density and degree of bone maturation. It is used to decide functional loading time and to estimate loading capability.

Ultimately, histologic or microscopic analysis serves as gold standard for evaluation of implant stability however major disadvantages exist due to its insensitivity and associated unnecessary or unethical invasive biopsy. [10] Therefore, various methods have been established to quantify implant stability in order to provide baseline information, to monitor the clinical outcome over the time course and to assess long term prognosis of an implant-supported restoration.

Resonance Frequency Analysis

Resonance frequency analysis (RFA) is widely accepted as a non-invasive method to determine implant stability at various time points after implant insertion. [3, 5, 10, 20] RFA has been introduced to provide an objective measurement of implant primary stability, to monitor implant secondary stability over the healing period [22, 23] or in the longer term follow up [24, 25] and to predict early implant failure. Peter Moy also stated its usage to improve success, to reduce treatment time, to avoid premature loading, to improve predictability with high risk patient and to determine time to proceed with definite restorations in his practice. [26] There are currently only 2 commercially available RFA units using different measuring approaches: original electrical method through direct wiring between the transducer and analyzer and the new magnetic device using magnetic frequencies between the two components.

Implomates (Bio Tech One®), an electronic-type machine for RFA, involves a transducer, consisting of an electrically driven rod to provide an impact force, attached to the implant of interest via screw attachment, in order to create the resonance response from the implant. The response signal, ranging between 2- 20 Hz, is then analyzed. The biggest amplitude represents the resonance frequency. The signal with high frequency and sharp peaks indicate a stable implant. [10]

Osstell (Integration Diagnostics AB, Gothenburg, Sweden) consists of 2 device generations. The former electronic machine (Figure 6A) involves an L-shaped transducer beam, attached to the implant of interest or abutment via screw attachment. This transducer contains two piezoelectric elements. The first vertical element generates a sinusoidal signal of 5-15 kHz, via its vibration to stimulate the implant or implant/transducer complexes while the other on the opposite side serves as a receptor for frequency and amplitude of the response signal from the implant. [10, 27, 28]

The former L shape of the transducer restricts its orientation clinically which adds a significant length to the exposed implant length. [10] Therefore, Osstell's later magnetic-type device was developed with a contact-free probe. (Figure 6B) A metallic rod with magnetic tip serves as transducer which is screwed onto an implant or implant

abutment. This magnet is then excited by a magnetic pulse from a wireless probe. After 1-ms-pulse duration, response signals are picked up by a receptor called a “smart-peg”, which vibrates freely, inducing an electric voltage in the probe coil or the resonance frequency analyzer. [4, 12]

With no transducer attached, the measurement is believed to be more accurate than the original electronic machine. Moreover, the contact-free design allows ISQ measurement from any direction. Due to these improvements, data derived from different device designs should be compared with caution. [10, 29] Although the electronic device and the magnetic device are capable of measuring similar changes, the magnetic device results in higher implant stability quotient (ISQ) value when measuring the stability of non-submerged dental implant. [12]

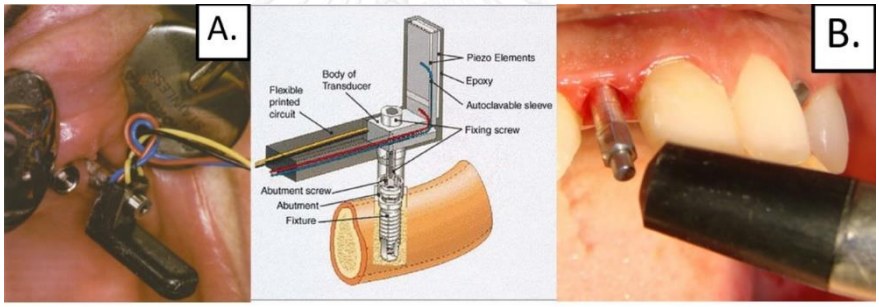

Figure 6. Resonance frequency analysis (RFA): component

A: Transducer connected to implant/abutment (electronic unit)

B: The contact-free probe (magnetic unit)

(Friberg, B., Sennerby, L., Meredith, N., and Lekholm, U. A comparison between cutting torque and resonance frequency measurements of maxillary implants: A 20-month clinical study. Int J Oral Maxillofac Surg 28 (August 1999): 297-303.)

(Gehrke, S. A., da Silva Neto, U. T., Rossetti, P. H., Watinaga, S. E., Giro, G., and Shibli, J. A. Stability of implants placed in fresh sockets versus healed alveolar sites: Early findings. Clin Oral Implants Res 27 (May 2016): 577-582.)

For both types of machine, the data was used to plot a Bode diagram, a plot of the amplitude against the frequency. [30] Resonance peaks from the received signal indicate the first flexural (bending) resonance frequency. [10] The frequency, corresponding with the highest peak in this plot, is chosen as the resonance frequency. [27, 30] Assuming an implant integrating to surrounding bone as one unit, the signal

response, representing the unit's stiffness, can be inferred to level of osseointegration. [10] The resonance frequency ranges between 3,500-8,500 Hz which is later translated, by Osstell, to implant stability quotient (ISQ) value of 0 to 100. [5, 10, 27, 28] This index is only valid for a specific type of implant in a human maxilla or mandible. For all other applications, the resonance frequency value should be used instead. [30]

It was shown that the device can sometimes mis-determine the resonance frequency value, especially when multiple peaks or a flat curve presented in the Bode diagram. In these situations, the highest peak is somewhat difficult to assign. Hence, clinical manual dictates that the measurement be discarded and redone when more than one peak is visible. [30]

The higher ISQ value indicates greater implant stability. [10] Therefore, RFA is used in monitoring treatment outcome and predicting early implant failure. According to manufacturer's guideline, ISQ > 70 represents "high stability", ISQ between 60–69 indicates "medium stability", and ISQ <60 is considered "low stability".

The ISQ value greater than 65 is suggestive of successful implant [10] and small ISQ value below 45 shows a risk of failure, especially with very low values at 2 months. A clinically mobile implant will give no resonance peak in return. [4, 10] Clinically, ISQ values of 60 to 80 are widely accepted as successful primary stability. At implantation appointment, ISQ values of at least 55 could represent clinical stability and possibly predict future successful osseointegration. [3, 4] Moreover, an ISQ value of 57-82 at 1 year, indicates implant success. For the determination of loading time, ISQ value of at least 70 is preferred for non-splinted implants. For immediate implant loading, an ISQ value of 60–65 is considered a good prognosis while ISQ < 52 is recorded as failure. [3, 4, 29]

Nedir and co-workers [31] investigated Osstell machine with ITI SLA implants in 2004 and recommended it as diagnostic tool capable of discriminating between stable and mobile implants using ISQ $\geq$47 as cut off point. An ISQ $\geq$49 at the time of placement were used as a predictive value for osseointegration when left to heal for 3 months. An implant with ISQ $\geq$54 is predictable to osseointegrate when immediately loaded.

In long-term evaluation, a significant decrease in ISQ was found after implant placement for several weeks as bone remodeling occurs, followed by a recovery to initial stage at the time of implant loading. [10, 32, 33] Softer bone can have a greater increase of ISQ value with prolong healing time. [20, 34]

However, there are some drawbacks of this methods. RFA can only give a reliable prediction of implant success, once osseointegration occurred. Implant with low ISQ value may undergo further healing process and obtains greater stability overtime. Thus, low ISQ should not be used as diagnostic criteria for implant failure unless longitudinal repeated measurements show no improvement. [10] Moreover, RFA can only be done in presence of the bone-implant interface so it cannot provide pre-surgical information for treatment planning and outcome prediction.

Factors Influencing Resonance Frequency Analysis

Implant mechanical properties and surrounding tissue characteristics were shown to influence ISQ value. These factors include implant length and diameter, effective implant length (length of exposed thread and abutment), implant surface, placement position, ratio of cancellous to cortical bone, bone density and damping effect of surrounding tissue. [3, 4, 10, 30, 32, 33, 35] Another important factor is difference in individual healing time. Therefore, to monitor long-term implant stability, series of intra-patient ISQ values over various time points is recommended.

1) Implant design

Kheur et al. [35] tested the effect of implant lengths and implant designs to find that longer implants had less ISQ values at implant placement step. Three possible explanations; A longer drilling time for long implant may lead to over preparation of implant site. Additionally, due to decreased diameter in the coronal portion of long implant, the marginal bone-to-implant contact reduced. [36] Lastly, as more number of implant threads move past the bone in longer implant, the area of bone with these repeated contact are subjected to deformation, leading to reduced stability. [35] However,

controversy exists as another study [37] reported an increase in ISQ in longer implant with a decrease in micro-movement.

For the thread design, asymmetrical cutting thread design showed lower ISQ than a propriety buttress thread. The possible reasons were a reduced pitch interval and a more apical tapered design which allows greater bone compression. [35] Additionally, implants with cervical microthreads exhibited significantly higher primary stabilities than those without. [33]

Implant diameter also has an influence on ISQ, with higher ISQ in wider implants. This effect was more pronounced at loading time than immediately after implantation. [3, 33] Furthermore, Gehrke et al. [33] stated that ISQ values were higher for the conical implants, comparing to the cylindrical ones.

2) Anatomical location

Huang et al. [3] conducted a retrospective study on possible factors influencing ISQ value. Immediately after implantation, ISQ was affected by maxillary/mandibular location. The mandibular implants showed more ISQ value than the maxillary ones. [3, 33, 38] It was stated that most implants in the maxilla had an ISQ less than 60 while those in the mandible had an ISQ greater than 60. [31] Nonetheless, there seems to be no intra-arch difference since similar stabilities were observed between maxillary anterior and posterior region. [33]

3) Bone quality

Tözüm et al. [32] measured ISQ of implants in three bone qualities (Figure 7), classified with mandibular cortical index (MCI) as followed; Class I: normal mandibular cortex, Class II: resorptive cavities in endosteal margin with cortical residues 1 to 3 layers-thick on one or both sides, and Class III: porous endosteal margin with thick cortical residues. The ISQ value of MCI class I were significantly greater than those of MCI class II and III at time of implantation and at 12-month follow up. Similarly, MCI class II also showed significantly greater ISQ value than MCI class III at both time points. ISQ value also showed a significant relationship with the Lekholm & Zarb index, another grading system for bone quality as well. [38] (Figure 8)

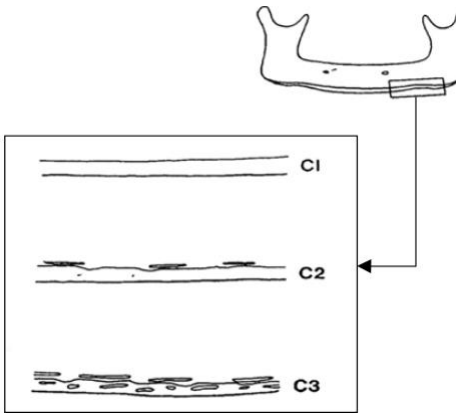

Figure 7. Mandibular cortical index. Showing 3 bone qualities of the endosteal inferior cortex on panoramic radiographs.

CI: Even and sharp margin on both sides of the mandible.

CII: Semilunar defects with cortical residues on one or both sides.

CIII: Thick cortical residues and clear porous.

(Marandi, S., Bagherpour, A., Imanimoghaddam, M., Hatef, M., and Haghighi, A. Panoramic-based mandibular indices and bone mineral density of femoral neck and lumbar vertebrae in women. J Dent (Tehran) 7 (2010): 98-106.)

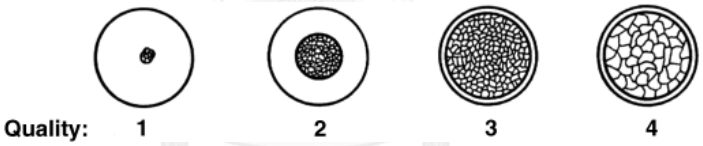

Figure 8. Grading for bone quality assessment (Lekholm & Zarb 1985).

Based on radiographic appearance and resistance at drilling, bone quality has been classified as:

Type 1: Almost the entire bone is composed of homogenous compact bone.

Type 2: A thick layer of compact bone surrounds a core of dense trabecular bone.

Type 3: A thin layer of cortical bone surrounds a core of dense trabecular bone.

Type 4: A thin layer of cortical bone surrounds a core of low density-trabecular bone of poor strength.

(Alsaadi, G., Quirynen, M., Michiels, K., Jacobs, R., and van Steenberghe, D. A biomechanical assessment of the relation between the oral implant stability at insertion and subjective bone quality assessment. J Clin Periodontol 34 (April 2007): 359-366.)

(Lekholm, U., Zarb, G. A., and Albrektsson, T. Tissue integrated prostheses. Chicago: Quintessence Publishing Co. Inc., 1985; 199-209)

Moreover, a retrospective study by Huang et al. [3] concluded that immediately after implantation (primary stability), ISQ was lower in bone grafted-patients and immediate implantation cases. The need for bone grafting indicated poor bone quantity and a smaller bone coverage of implant thus lowered the ISQ value. These effects are not significant at immediately before implant loading time. Thus, with careful case selection, immediate implantation can be done without significant decrease in secondary stability. In the same trend, Gehrke et al. [33] also stated that immediately placed implants yielded lower ISQ values, compared to implants placed in healed site.

Although differed in primary stability, both mandibular and maxillary implants developed more ISQ over time in a similar manner, implying that the discrepencies were based on different bone density rather than the differences in osseointegration process. [3]

4) Peri-implant condition

Pattijn et al. [30] studied resonance frequency measurement in the guinea pig model. They reported the influence of type of boundary condition and the length of bone on the resonance frequency values. The larger bone around implant site was shown to lower the ISQ since greater deformation was allowed. They also stated that the presence of soft tissue lead to higher stiffness of the bone–implant–transducer system in vivo.

5) Orientation of transducer

Pattijn et al. [30]used RFA in the guinea pig model and reported the influence of transducer orientation on the resonance frequency values. The orientation of transducer is classified as perpendicular or parallel to the long axis of the bone. In case where the bone has higher compressive deformation resistance, the ISQ is believed to be lower with the perpendicular transducer. The opposite effect goes for the bone with higher bending deformation resistance. However, ISQ was found unaffected by site of measurement (labial, lingual, distal, and mesial sites). [3]

Insertion Torque

Torque is a turning force toward an object. Insertion torque (IT) is defined as a force used to insert an implant into a prepared osteotomy, expressed in Ncm (Newton centimeter) units. This force is generated by the placement force from the tip of instrument, combined with the friction as the implant pass through bone. [18] IT can be subjectively estimated by experienced surgeons or quantitatively measured with an electronic devices coupled with physio-dispenser or with a torque gauge incorporated with manual ratchets. [18, 20] (Figure 9) The peak IT is obtained near the final seating step due to the force between the implant's butt against the bottom bone of the recipient site and the contact of the implant flange with crestal bone, combined with interfacial stress along the implant surface. [20, 27]

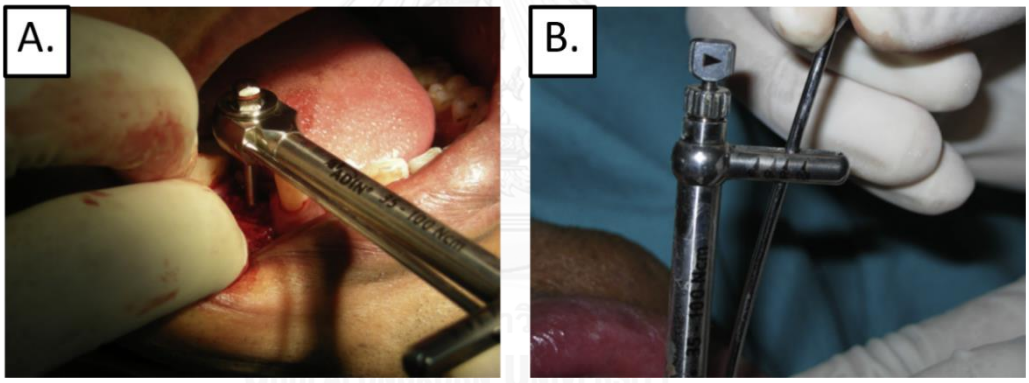

Figure 9. Insertion torque measurement

A: Implant being placed with manual ratchet. B: A torque gauge

(Goswami, M. M., Kumar, M., Vats, A., and Bansal, A. S. Evaluation of dental implant insertion torque using a manual ratchet. Med J Armed Forces India 71 (December 2015): S327-332.)

Insertion torque can be used to imply the bone quality as bone density and hardness, by determining the amount of force needed for implantation. Additionally, it is also used in assessing implant primary stability and in deciding the loading protocol. Implant with high IT obtains a higher primary stability, compared to implant with lower IT which can lead to implant failure.

Studies have indicated IT near the range of 35 Ncm to be satisfactory. For immediate implant loading, implant manufacturers have provided an optimal IT range to be achieved to avoid over-compression or for the metallurgical reasons. [18] Over-compression can cause an adverse effects on bone healing. Angiogenesis is impaired under high stress, leading to hypoxia with a reduction of bone formation in the peri-implant region, thus decreasing implant stability. [39] High stress also affects bone cells with reduction in osteocytes and increase osteoclastic activity, resulting in bone destruction. [40]

Insertion torque measurement can only be performed during implant insertion time hence neither pre-surgical information nor longitudinal data, for implant planning and monitoring, can be obtained. Therefore, its primary use lies in assessing implant primary stability. [10]

Factors Influencing Insertion Torque

Many factors are shown to have influences on IT, including the bone density and hardness, drilling diameter, implant design and anatomical location. [18, 38]

1) Bone density

According to Misch bone density classification, bone density levels in the edentulous area can be divided into 4 groups. (D1-D4, Table 2). IT value was found to be associated with bone density with the highest IT, detected in D-1 type bone and the lowest in D-4 bone. [18] IT value also showed a significant relationship with the Lekholm & Zarb index, another grading system for bone quality. [38] (Figure 8) Ostman et al. [36] also reported a lower implant stability with decreased bone quality. This finding was believed to be associated with the amount of cortical bone present, since it is more stiffer than trabecular bone. In agreement with previous study, Friberg et al. concluded that a significant correlation between IT and RFA was found only at the upper/crestal third of bone portion, hence supported the importance of marginal bone in implant stability. [34]

BONE DENSITY	DESCRIPTION	TACTILE ANALOG	TYPICAL ANATOMICAL LOCATION
D1	Dense cortical	Oak or maple wood	Anterior mandible
D2	Porous cortical and coarse trabecular	White pine or spruce wood	Anterior mandible Posterior mandible Anterior maxilla
D3	Porous cortical (thin) and fine trabecular	Balsa wood	Anterior maxilla Posterior maxilla Posterior mandible
D4	Fine trabecular	Styrofoam	Posterior maxilla

Table 2. Misch bone density classification scheme

(Misch Carl, E. Bone density: A key determinant for treatment planning[Online]. 2015. Available from : http://pocketdentistry.com/7-bone-density-a-key-determinant-for-treatment-planning[2017,July 18])

2) Drilling dimension

The under-dimensioned drilling comparing to the implant diameter, and tapered implant design helps increasing IT. Both share similar aim to cause local compression.

Campos et al. [41] studied effect of different drilling dimension on IT value in a dog radii. They concluded that IT was inversely proportional to the drilling dimension. Different degree of under-dimensioned drilling resulted in different initial healing pathway. The smaller drill yielded intimate contact between implant surface and drilled walls immediately after placement. These regions underwent appositional bone healing pathway where bone necrosis occurred hence implant stability falls for a period of time, until the secondary stability is achieved, following bone remodeling and new bone formation. For larger drills, healing chamber was present between bone-implant surface, resulting in lower primary stability. The chamber area was later evolved to a connective tissue scaffold for bone healing via intramembranous-like ossification. There was no extensive necrotic bone spots since compression was relieved. Thus, larger drills accomplished faster woven bone gap filling, in other word, more rapid secondary stability gain. Although smaller drills gave higher IT and primary stability, after bone necrosis began, the bone-to-implant contact later reduced to the level comparable to a healing chamber.

3) Implant design

Tapered implant design is superior in generating compression, comparing to parallel implant design. Since its gradually increased diameter allows continuous lateral

bone compression along the entire implant length, the IT value increases as well. [18] However, reduction in IT was reported in implant which incorporated cutting edges. [20]

4) Anatomical location

Alsaad et al. measured IT of 720 oral implants and found that mandibular site gave a higher IT value, especially in symphyseal area. The lowest IT value was detected at posterior maxilla. Significant difference in IT was also detected between anterior and posterior jaw location. [38]

Fractal Property and Fractal Analysis

The word "fractal" has been used to describe an entity with self-similar form, a property in which a magnified subset is indistinguishable from the whole object as shown with samples in Figure 10 & 11. [42-44] Therefore, their metric properties (such as length, perimeter or area) depend on the magnification and size of the spatial scales or iterations as clear seen in Figure 11b. [43, 44]

Basic terminology needed to understand fractal dimension (FD) is **Hausdorff-Besicovitch dimension** (D_h), which for this study refers to measurements of the space. It can be calculated as the logarithmic ratio, between the number of an object's internal homotheties (subunits with similar pattern) and the reciprocal of the common ratio (r) of this homothety. [43] (Figure 10C & 11C)

Figure 10. Fractal object "Sierpinski sieve"

A. The magnified subsets always has overall shape of an equilateral triangle.

B. Resulting in a triple copies when double its side dimension

C. Hausdorff- Besicovitch dimension = log (3)/log(2) = 1.585

Figure 11. Fractal object “Koch snowflake, Koch curve or Koch island or Koch star”

A. The magnified subset always has an equilateral triangle in middle 1/3 of each sideline.

B. Resulting in an increasing side by a factor of 4 or $N_{n-1} \cdot 4$ after n iterations, the sidelength of $\frac{S_{n-1}}{3} = \frac{s}{3^n}$, increasing perimeter length of $N_n \cdot S_n$, an increasing of area of $a_0\left(1+\frac{3}{5}\left(1-\left(\frac{4}{9}\right)^n\right)\right) = \frac{a_0}{5}\left(8-3\left(\frac{4}{9}\right)^n\right)$ when a_0 equals original area

C. Hausdorff- Besicovitch dimension = log (4)/log(3) = 1.26186

In mathematics, there are several ways to define the space. The most accustomed one is topological space or space with integer D_h. Of which, the topological dimension (D_T) of a point is 0. A line has dimension of 1. A plane has dimension of 2, and a volume has dimension of 3. For an object with non-integer D_h (D_h is greater than its topological dimension) is referred as fractal object. [43]

The concept of fractal analysis (FA) arises in order to quantify the complexities of the objects with internal heterogeneity or irregularity. [44] These variability cannot be explained by traditional Euclidean topology. For instance, both straight line and serrated line has the same constant topological dimension of 1, but fractal geometry accounts for this difference since, in fractal geometry, the Euclidean concept of ‘‘length” is viewed as a process of varying scaling sizes (different length) rather than an event of the line. [43] This phenomenon is often expressed by spatial or time-domain scaling laws with the power-law behavior (log-log plot). Various algorithms have been raised to calculate fractal dimension (FD), a quantitative parameter of complexity degree. [42, 43]

The main concept of these FA methods consists of three basic steps; the first step is to measure the quantities of the object with various scaling sizes (mostly length, surface or volume). Next, regression line is fitted into a power-law plot of log (measured quantities)

versus log (step sizes). Lastly, the FD is calculated from the slope of this regression line. [42, 43]

Among a variety of methods for estimating the FD, they can be classified into 3 categories; simplified spatial methods, general spatial methods and spectral methods. [42]

1) **Simplified spatial methods**

Simplified spatial methods analyze FD values based on binary image, created from image segmentation where images of bone are divided into foreground and background. The borderlines of these segmentations are considered as a curve for FD measurement. [42]

Morphological image processing is operated to remove the imperfections by accounting for the form and structure of the images since binary images, derived from thresholding, may contain some noise. Morphological techniques place a template of small binary image with a value of 0 or 1, called a structuring element, at each pixel in the image and compare the element with the corresponding neighborhood of pixels. The element is defined as "fit" to the image if each of its pixel with a value of 1 also has the corresponding image pixel with a value of 1. If there are only some amount of pixels that pass this condition, the element is defined as "hit". (Figure 12) Fundamental operations are as followed.

		A	B	C
fit	s_1	yes	no	no
	s_2	yes	yes	no
hit	s_1	yes	yes	yes
	s_2	yes	yes	no

Figure 12. Examples of fitting and hitting of the structuring element s_1 and s_2

(Morphological image processing lecture notes follow chapter 11 of textbook: digital image processing: A practical introduction using java™[Online]. Available from : https://www.cs.auckland.ac.nz/courses/compsci773s1c/lectures/ImageProcessing-html/topic4.htm[2017,July 18])

Erosion and its variants (Figure 13): Erosion is the process where the origin of the structuring element is placed to each image pixel. The new binary image is produced following a rule that the image pixel value is set to 0 unless the element fit to the corresponding image. Erosion shrinks an image, expands the gap between regions and removes the pixel with weak link.

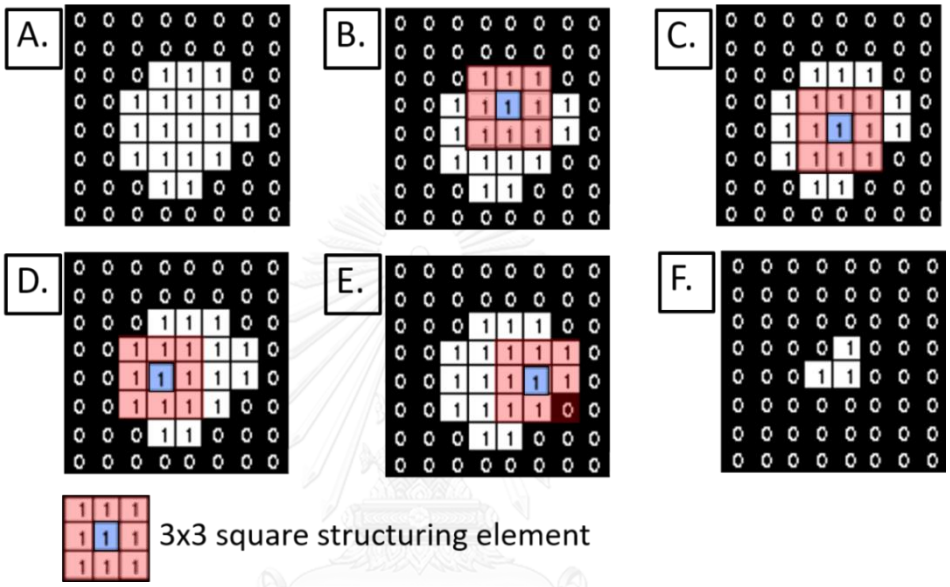

Figure 13. Erosion process; A: Original binary image, B-D: "Fitting" of the structuring element, only these 3 pixel images, which superimpose with the element's origin, are kept intact, E: Example of "hitting" of the structuring element, this pixel image value is set to 0, F: Resultant image.

(Adapted from: Morphological image processing lecture notes follow chapter 11 of textbook: digital image processing: A Practical introduction using java™[Online]. Available from : https://www.cs.auckland.ac.nz/courses/compsci773s1c/lectures/ImageProcessing-html/topic4.htm[2017,July 18])

Shrinking is a variant of erosion where a single-pixel is left intact, so the total object count remains the same. Another variant is **thinning** where the pixels are retained if their removals result in destroying connectivity of a region. Illustrated images are shown in Figure 14.

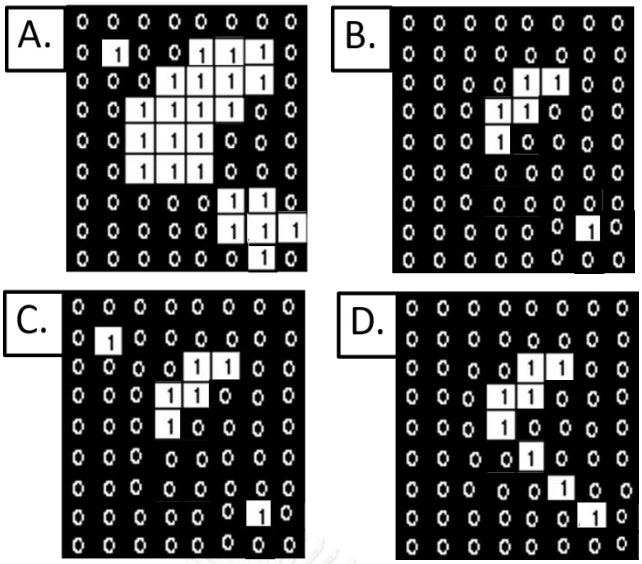

Figure 14. Comparison between erosion and its variants.

A: Original image B: Erosion C: Shrinking D: Thinning

(Adapted from: Morphological image processing lecture notes follow chapter 11 of textbook: digital image processing: A Practical introduction using java™[Online]. Available from : https://www.cs.auckland.ac.nz/courses/compsci773s1c/lectures/ImageProcessing-html/topic4.htm[2017,July 18])

Dilation and its variant (Figure 15): Dilation of an image produces a new binary image by setting the value of all corresponding image pixel to 1 when the element hit the original image pixel. Otherwise, the pixel value is set to 0. Dilation is an opposite process to erosion. It expands an image by adding a layer of pixels to the boundaries of regions. Dilation also smoothens small negative regions and fills in the voids. **Thickening** is a variant of dilation that do not allow merging of nearby objects. (Figure 16)

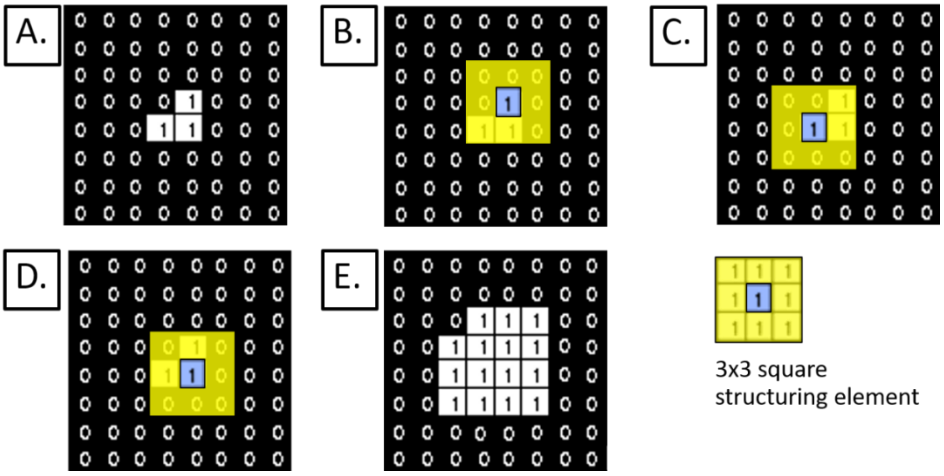

Figure 15. Dilation process.

A: Original binary image, B-D: “Hitting” of the structuring element, all corresponding image pixel values, in the yellow area, will be set to 1, E: Resultant image.

(Adapted from: Morphological image processing lecture notes follow chapter 11 of textbook: digital image processing: A Practical introduction using java™[Online]. Available from : https://www.cs.auckland.ac.nz/courses/compsci773s1c/lectures/ImageProcessing-html/topic4.htm[2017,July 18])

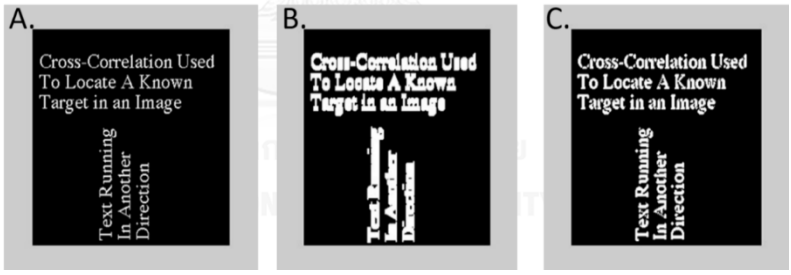

Figure 16. Comparison between the effect of dilation and thickening

A: Original image, B: Dilation, C: Thickening

(Ursula, T. Chapter 18 Image segmentation[Online]. 2016. Available from : http://slideplayer.com/slide/6610087/ [2017,July 18])

Compound operation of an erosion followed by a dilation is called **opening**. (Figure 17b) It eliminates small islands and thin bridge of pixels, resulting in a gap between objects. Any remaining regions are restored to their original size by the dilation. **Closing** is a dilation followed by an erosion. It helps filling holes in the regions, in other word, removing islands and thin filaments of background pixels while keeping their initial sizes. (Figure 17C)

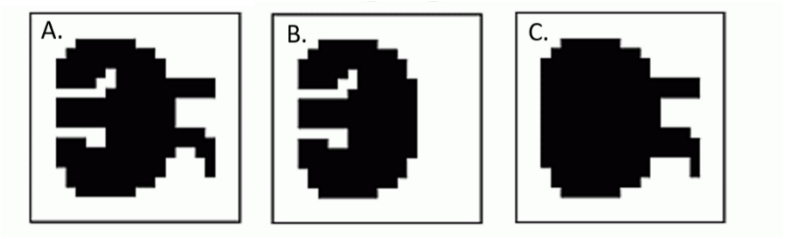

Figure 17. Effect of opening and closing process.

A: original image B: opening C: closing

(Smith Steven, W. The Scientist and Engineer's guide to digital signal processing by Steven W. Smith Chapter 25-special imaging technique/ morphological image processing[Online]. California Technical Publishing, Available from : http://www.dspguide.com/ch25/4.htm[2017,July 18])

Skeletonization (Figure 18) erodes the image equally from all directions until only the central line of pixels remains. The element placement and erosion follow four basic rules. First, the element is placed on an image pixel that has a value of 1. Secondly, at least one of that pixel's close neighbors must have a value of 0 to insure that the erosion takes place from the outer border. Thirdly, the pixel will not be removed if only one of its neighbor has a value of 1 since this is indicated as the end of a line. Lastly, a pixel will also be kept if erosion results in its neighbors being disconnected. This is in order to construct a continuous line.

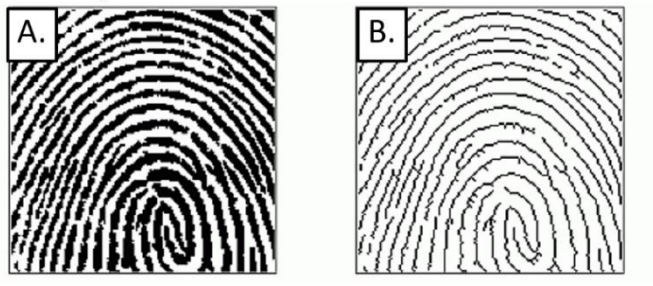

Figure 18. The effect of skeletonization

A: Original image B: Skeletonized image

(Smith Steven, W. The Scientist and Engineer's guide to digital signal processing by Steven W. Smith Chapter 25-special imaging technique/ morphological image processing[Online]. California Technical Publishing, Available from : http://www.dspguide.com/ch25/4.htm[2017,July 18])

After morphological binary image processing, the FD is calculated from the resultant image by one of the following scales.

1.1) **Caliper method** (Figure 19), the best known method to measure FD of curves, measures the length (L) of the borderline as a function of a span (S). Then, a log-log plot is made of L against S and FD is calculated from a slope of the obtained regression line. [42]

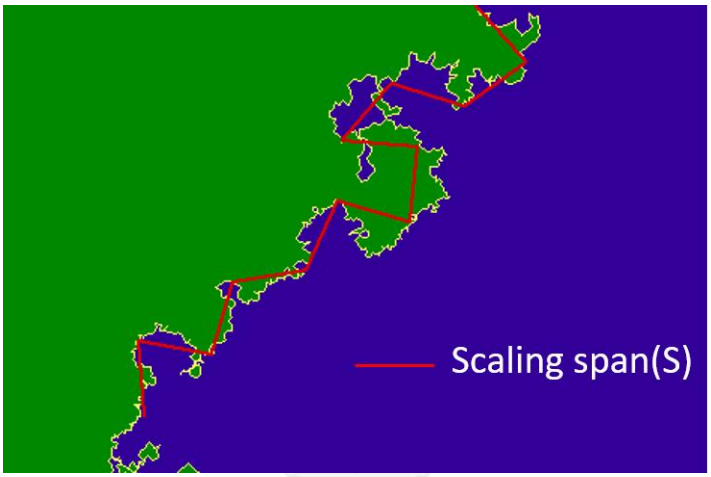

Figure 19. Caliper method. Measuring the coastline (L) with a span (S)

(Center for polymer studies. Fractal coastline[Online]. Physics department and Science and mathematics education center Boston University, Available from : http://polymer.bu.edu/ogaf.html[2017,July 18])

1.2) **Tile counting method** or Mosaic amalgamation method (Figure 20A) is an expansion from Caliper method. Instead of a caliper span, the square grids with increasing edge length (S) are superimposed on the image. The number (N) of the tiles contacting the boundary is counted. A log-log plot is plotted with N against S. Then, the FD is again calculated from the slope of the fitted straight line. [42, 44]

There is another adjusted version, the Modified tile counting method (Figure 20B), also referred as box counting method, in which the total number (M) of tiles covering the foreground is analyzed and used to create a log-log plot of M against S. [42, 43]

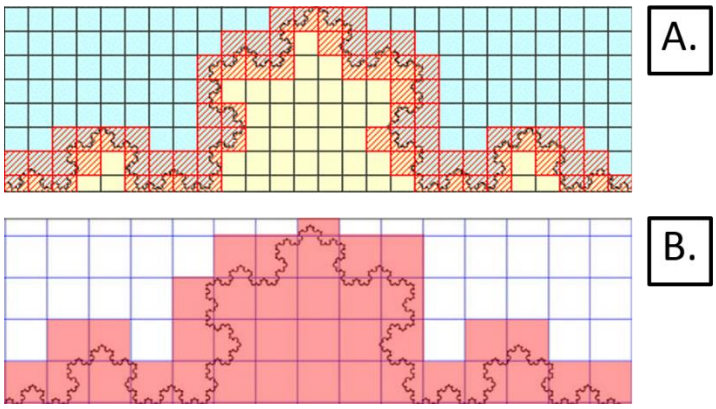

Figure 20. Demonstrate the Tile counting method (A) and the Modified tile counting method (B)

(Sánchez, I., and Uzcátegui G. Fractals in dentistry. J Dent 39 (April 2011): 273-292.)

(Dimension by box-counting[Online]. Available from : http://users.math.yale.edu/public_html/People/frame/Fractals/Labs/CoastlineLab/CoastlineLab.html[2017,July 18])

1.3) **Extended counting method** (Figure 21) is an alternative to the tile counting method. The image is divided into many subsets which is further operated by tile counting method. The maximum of the subset dimension is considered as FD. Thus, this FD is obtained from the most complex region. [43]

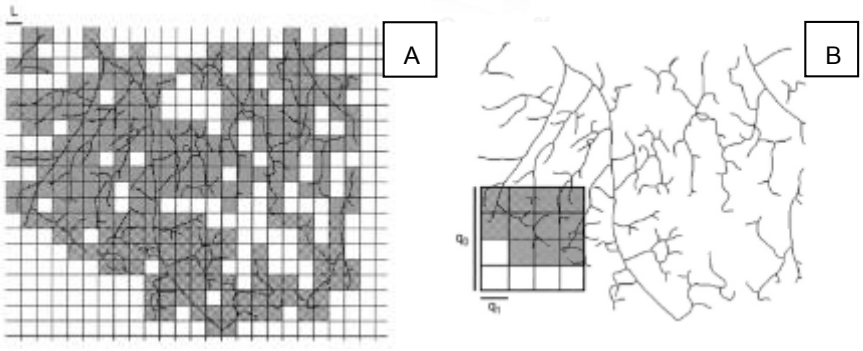

Figure 21. Tile counting method (left) and Extended counting method (right)

A. Using a grid of boxes of the size of the network and count every gray box

B. Using a grid of boxes smaller than the size of the network

(Hermán, P., Kocsis, L., and Eke, A. Fractal Branching pattern in the pial vasculature in the cat. J Cereb Blood Flow Metab 21(2001): 741-753.)

1.4) Pixel dilation method (Figure 22) starts by converting the foreground to an outline of one-pixel width. The images then undergo repeated dilation with circular structuring elements of various widths (W). The length (L) of the dilated outline is estimated for each W used in the dilation step. A log-log plot is made with L against W. A straight fitted line is generated and its slope is obtained for FD calculation. In the modified pixel dilation method, the area of the foreground is measured rather than the length. The ratio (N) of foreground area to the structuring element area (E) is observed. A log-log plot of N against E is further created. [42]

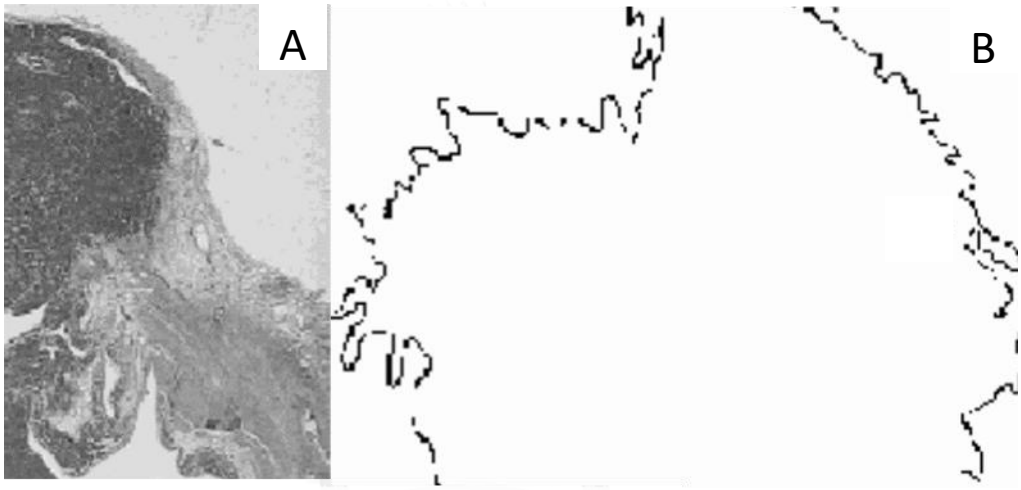

Figure 22. Determining the FD of the cross-sectional infarct scar edge

A: Histologic trichrome stained section of rabbit myocardial infarction

B: X10 edge detection used for FA

(McLachlan, C. S., et al. A method to determine the fractal dimension of the cross-sectional jaggedness of the infarct scar edge. Redox Report 5 (2000): 119-121.)

2) General spatial methods

General spatial methods are based on generating an image surface. The two dimensional images are converted to three dimensional surface by letting the intensity or optical density of each pixel represent the elevation of the surface as a distance in the third dimension. [42] (Figure 23) Therefore, these methods can be used in grey–scale images thus eliminate the need for image segmentation. [43] The method for FD

measurement on a three dimensional surface are operating in the spatial domain. A true fractal surface is scale independent, meaning that the structure is similar on every scale including the intensity dimension. [42]

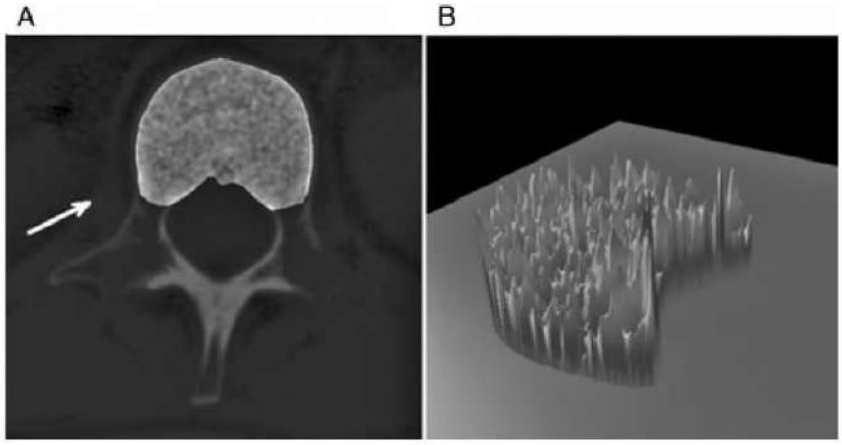

Figure 23. Example of an image intensity surface.

A: A cross-sectional computed tomographic image of a vertebra.

B: Elevation landscape of the segmented spongy area. The white arrow indicates the view direction.

(what-when-how homepage. Estimation techniques for the fractal dimension in gray-scale images (Biomedical image analysis)[Online], Available from : http://what-when-how.com/biomedical-image-analysis/estimation-techniques-for-the-fractal-dimension-in-gray-scale-images-biomedical-image-analysis/[2017,July 18])

2.1) Box counting method calculates the image surface area (A) of the original image at finest scale approximation. Then, the image is coarsened repeatedly with various scale approximation (S) to reduce the resolution. The image surface area is measured for each coarsening process. The obtained data are used to construct a log-log plot of surface area (A) against window size (S). [42]In the modified box counting method the number (N) of cubes with side length (S), needed to cover a fractal surface, is counted and a log-log plot of N against S is created.

2.2) Differential box counting method (Figure 24) is an adaptation of the box counting method. The image surface is partitioned into boxes of various edge length (r). The number (N) of boxes needed to cover the minimum and the maximum intensity levels

in each area (r x r) is counted. A log-log plot of N against r is created and used in FD calculation. The method is box size sensitive. With too large box size, the number of boxes would be much less than the number of intensity levels. For too small box size, there would be too many boxes above the grid that are unaccounted which lead to underestimated FD. [43]

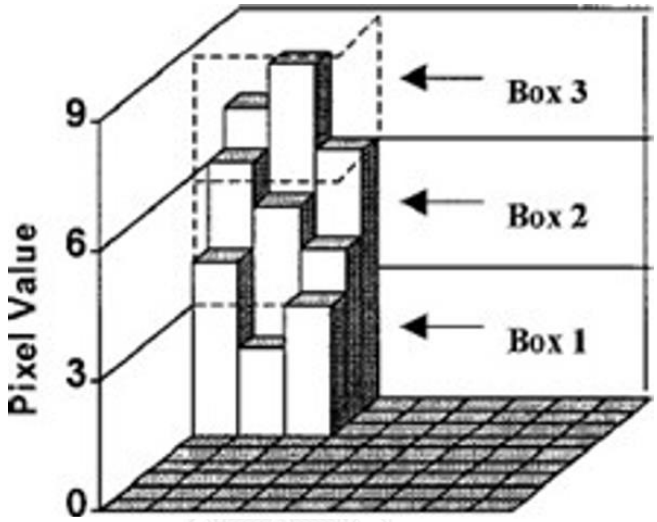

Figure 24. Differential box counting method. In this area of r x r, the number of boxes, needed to cover the minimum intensity (Box.1) and the maximum intensity levels (Box.3), equals 3 boxes.

(Wachirahatthapong H. An improved triangle box counting method for fractal dimension estimation[Online], Atitarn B, 2015. Available from : http://slideplayer.in.th/slide/2729231/[2017,July 18])

2.3) Triangular prism method (Figure 25) creates an image surface with triangular prisms. A number of grids at various scale size, needed to cover the surface area, is examined. A log-log plot of number of grids against the scale size is generated. [43]

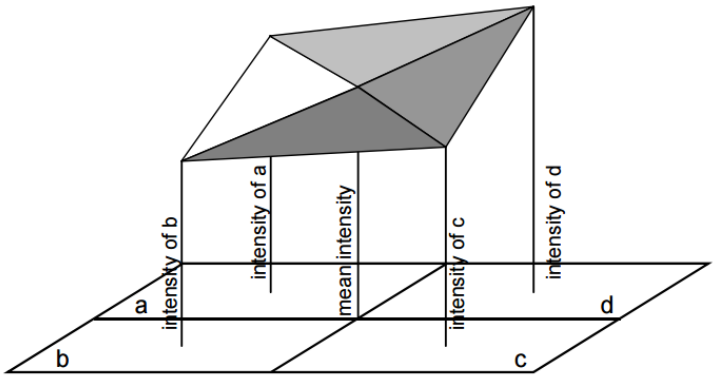

Figure 25. Triangular prism method for calculating fractal dimension.

(Quackenbush, L. J. Calculating fractal dimension using the triangular prism method. In Proc. ASPRS 2005 Annual Conference[Online]. 2015. ,Available from : ftp://ftp.ecn.purdue.edu/jshan/proceedings/asprs2005/Files/0144.pdf[2017,July 18])

2.4) **Intensity variance method** (Figure 26) evaluates the intensity difference between any two points at a distance (S) from each other. The variance (V) or standard deviation of image intensity is calculated for every distance (S). Then, V is plotted as a function of S. The slope of the fitted straight line is used for further FD calculation. [42]

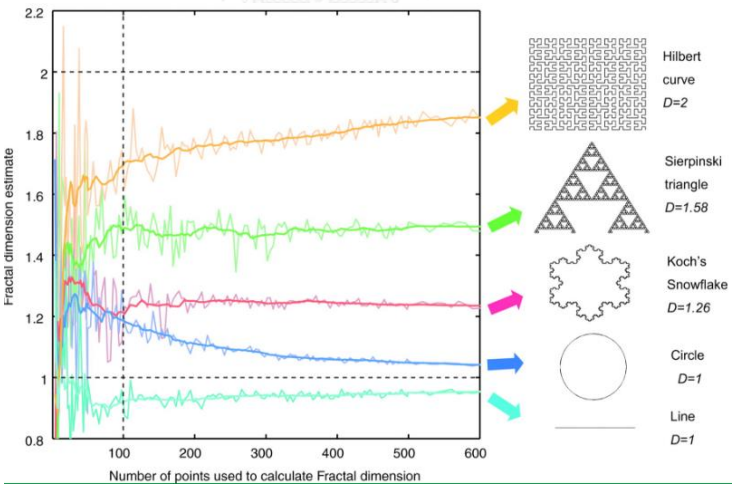

Figure 26. Intensity variance methods of 5 datasets of known theoretical fractal dimensions

(Tremblay, Y., Roberts, A. J., and Costa, D. P. Fractal landscape method: an alternative approach to measuring area-restricted searching behavior. Indian J Exp Biol 210 (2007): 935-945.)

2.5) **Hurst method** scans the image surface to find the greatest difference (M) between any two points within a distance (S). For normalization, M is divided by the

standard deviation of the elevation data. The slope of the line fitted to the plot of M as a function of S is used to calculate for FD. [42]

2.6) **Variation method** examines the maximum difference in intensity within the neighborhood of a pixel. For a circular neighborhood, the shape is expressed by its radius. In case of a square neighborhood, the edge length is defined. Total variation (V) is calculated from the sum of all maximum differences for each pixel in its neighborhood. A log-log plot of V against the size of the neighborhood (L) generates a straight line with a slope to calculate for FD. Sometimes, the vertical scale is normalized, as described in the Hurst method. [42]

2.7) **Blanket method**, a modification of the variation method, considered the area (A) of the image intensity surface. Two blankets are created at the brightest and darkest intensity level of any pixel in the neighborhood. The volume (V) between these two blankets is calculated for each size (L) of the neighborhood. The image intensity area (A) is defined as [V(L)-V(L-1)]/2. A log-log plot of A against L is made and FD is calculated from the slope of the fitted line. [42, 43]

3) **Spectral methods**

Unlike the methods described above which operate in the spatial domain, spectral methods operate in the frequency domain, using the Fourier power spectrum. Power spectrum method uses the two-dimensional Fourier transformation of the digital image. [42] Each image line is Fourier transformed and the power spectrum is evaluated. [43] The power spectrum (P) varies with frequency (F). A log-log plot between P against F is constructed and the slope of the line is used in FD calculation method.

Fractal Bone Analysis

Fractal geometry can be used in diagnostic interpretation of medical images as it offers a parameter to explain texture composition of the image, a key component in image pattern recognition and identification of possible abnormality. The images often exhibit certain similarities at different spatial scales which cannot be demonstrated clearly on a finite resolution image. [43, 44]

A wide variety of images in dentistry can be assessed with FA, including dental radiographs, ultrasonic images, sialographs, and histological sections. [44] Among many applications of FA, bone trabecular architecture, one of the most important factors contributing to bone strength, has been analyzed, usually with tile counting method. [5, 43, 44] The use of fractal analysis in this field is considered valid since cancellous bone has been shown to possess self-similarity property and magnification-dependent metric property. [45] FD value of trabecular bone from radiographs ranges between 1-2, the value indicating dimension between linear structure and a plane, respectively.

FA measures the complexity of trabeculae. Therefore, any condition which altered the internal structures of bones, should result in FD discrepency. [5] Hence, fractal analysis is currently applied in image discrimination, between healthy and abnormal bone group such as detection of osteoporosis, periodontitis, and hyperparathyroidism. They can also be applied in treatment and healing monitoring, for instance, in dental implant treatment, root canal therapy and orthognathic surgery. [42, 44] FD helps detecting early loss of bone quality and monitoring alveolar bone regeneration.

Tolga Suer, B., et al. [5] measured pre-surgical FD of posterior mandibular bone on panoramic radiograph, using modified tile counting method. The results were shown to correlate with both ISQ (R^2=0.1344) and IT (R^2=0.2045) at implant placement time. Similarly, Lee et al. also reported a significant correlation between FD from panoramic radiographs and ISQ in combined jaw group and only mandible group (R=0.400 and 0.571, resepctilvely), but not for the maxilla group (R=0.0350). [28] These findings support the possible use of pre-surgical FD in predicting implant primary stability. Veltri et al. [27] assessed the biomechanical parameters of 16 implants in rabbit femurs and concluded that FD from modified tile counting method, was correlated with IT value (R^2=0.447). However, there is no correlation between FD and ISQ values, which was inconclusive due to small sample size. According to receiver operating characteristic or ROC analysis, a fractal dimension breakpoint of 1.83 could be used to predict, with a sensitivity of 80% and a specificity of 88%, of the final IT $\leq$ 10 Ncm, which is the IT value indicative of bone quality type 4 according to Lekholm & Zarb classification. [38]

Factors Influencing Fractal Dimension Value from Radiographs

1) X-ray parameters

Shrout et al. [46] used a caliper method to calculate FD of the interdental bone of hemimandibles, from digitized radiographs with 4-6 degree variation in beam alignment and an approximate 5-fold variation in exposure time (0.2, 0.6 and 1.0 seconds). The FD was found to be insensitive to all of these variations. However, greater FD was observed with the longest exposure time and a power calculation indicated that effect of exposure might be significant in a larger sample size.

In agreement with previous study, Jolley et al. [47] studied FD from Fourier transform fractal analysis of periapical radiographs in maxillary incisor area of dry skulls and concluded that FD was not affected by variations in angulation, ranging from -10 to +30 degree with respect to occlusal plane. Alteration in tube potential, ranging from 50 to 80 kVp, and variations of impulse, ranging from 4 to 12 impulses, did not cause significant difference in FD calculation as well. Additionally, the differences in FD from different setting was much smaller than the difference among different skull at the same setting. This finding implied that the discrepancies in FD value from technical factor alteration may be relatively insignificant. Ruttimann et al. [48] also confirmed that FD of the interradicular mandibular bone, derived from power spectral method, is angular independence within a range of 10 degree.

Güniz Baksi et al. [49] also studied the effect of 3 exposure time variations (0.05, 0.12, 0.3 seconds) on FD calculation, using differential box counting method on digital periapical radiographs of dry human mandibles. Contrary to previous studies, FD values were shown to decrease with increase in exposure time. This decreased FD was presumed to result from a decrease in image noise with higher exposure. Thus, it could be assumed that non-standardized intra-oral radiograph could be used for determining and comparing FD values if the exposure parameters were fixed.

For cone beam computed tomography (CBCT), Pauwels et al. [50] concluded non-significant effect of the kV value on FD in cylindrical bone samples, in case that the radiation dose was kept at constant level. However, kV affects the relative amount

of scattered radiation and may lead to image noise. It was suggested that an increase in noise may not significantly affect bone segments but more pronounced effect of kV is suspected in larger samples.

2) Region of interest (ROI) selection

Shrout et al. [46] had shown that FD of the interdental bone from digitized radiographs, calculated with a caliper method, was not affected by a non-standardized ROI placement when the ROI size and shape was limited by crestal bone and adjacent roots. The same authors also studied the effect of ROI size on FD of the interdental bone from bitewing radiographs, using caliper method. Their results showed smaller FD with a large ROI; however, their ROI included small portion of tooth. [51] Additional area apart from object of interest can cause alteration in FD value thus ROIs placement should include the same structures in all images. These results implied that a specified ROI placement might not be necessary, on condition that no adjacent lamina dura, periodontal ligament space and root surfaces are not included.

3) Anatomical location

Bollen et al. [52] compared FD from periapical radiographs and found that FD measured in mandible was lower than in maxilla. Geraets and van der Stelt [42] also explained the contradictory outcomes in FD calculation, regarding osteoporotic bone as a result from difference in anatomical sites and imaging method.

Ruttimann et al. [48] analyzed FD of the interradicular bone of human mandible in vitro, using power spectral method. The results showed significant differences among different anatomical location with the highest FD at molar region and a relatively small difference between incisor and premolar area. Huh et al. [53] also studied FD value in dry mandibles, using the modified tile counting method. The largest FD value was shown in the angle region, while the least value was at the incisor region. Both sites demonstrated significant FD differences from the molar and premolar regions. The differences in trabecular structure were speculated to be the responsible factor for this finding. Since the angle bone showed thin and complex trabecular structure, whilst the incisor region showed thick and simple structure. Moreover, Oshida et al. [54]

measured FD of a mandibular cadaver and concluded that dentulous mandible gave higher FD than edentulous mandible.

4) Imaging modalities

Bollen et al. [52] reported that FD, measured on panoramic radiographs, were lower than FD on periapical radiographs. Lower resolution of panoramic radiographs may be responsible for this finding since finer bony structures are captured only on periapical radiographs. Therefore, overall greater trabecular thickness, shown on panoramic radiographs, could lead to lower FD value. Another possible cause is the difference in exposure technique. A panoramic radiograph is in essence a tomogram thus it is less influenced by cortical bone, whereas periapical radiograph projects the radiation through both cortical and trabecular bone. Tolga Suer, B., et al. also mentioned concerns about cortical superimposition on panoramic radiograph and the effect of different filtering steps on FD. [5] Another difference is in the ROI location. In panoramic radiograph, area beneath the root was chosen rather than the interdental bone, due to anatomical limitation. However, both methods follow the same changes in response to differences in bone quality.

Pauwels et al. [55] compared image quality between a wide range of CBCT devices, using a cylindrical polymethyl methacrylate phantom with two types of inserts, containing a line-pair and rod pattern. A wide range of image quality was shown resulting from difference in spatial resolution, contrast resolution, noise, and geometric accuracy. This inconsistency in image quality between CBCT devices might affect in FD calculation.

Furthermore, difficulties exist in identifying the correct threshold for image segmentation in CBCT images. CBCT grey values are influenced by the partial volume effect (PVE). [56] The voxels that contain both bone and marrow information will have an ambiguous grey value between that of bone and marrow. Thus, it is difficult to determine that voxel as foreground or background. With large voxel sizes, the influence of PVE can result in thicker trabeculae or loss of thin trabeculae which might lead to FD alteration. [57]

5) Algorithms used to calculate the fractal dimension

Even though various methods share similar basis in FD calculation, they are not mathematically identical and give different FD values [43] unless an ideal fractal objects, which contain continuous information and true self-similarity, was measured. However, digitized pixel data are sampled rather than continuous and self-similarity in bone is confined to the scale sizes between about 0.1 mm and 5 cm. [42] Additionally, different thresholding techniques, used to convert original image to binary image, could have a large effect on the amount and structure of bone retained on the image and the amount of noise. [50] Therefore, in order to compare the true difference in FD value, the choice of thresholding technique and calculation algorithms should be standardized.

Although trabecular bone contains the fractal property, its self-similarity limits to a specific range of scale, influenced by the structural and functional properties. [53] An overall size of the object places an upper limit of applicable scales. A lower limit is set by the spatial resolution or the pixel size that made up the image. [42] To determine the true FD, an optimal range of scales is needed. Huh et al. [53] studied the effect of tile sizes on FD value of human dry mandibular trabeculae, in angle, molar, premolar, and incisor regions, using the modified tile counting method. They reported the optimal range of tile size between 0.132 – 0.396 mm with the upper limit almost coincided with the mean trabecular thickness. They also discussed that in the lower ranges of scales, the FD calculation is restricted by the limitation of image resolution and high frequency noise while in the higher ranges, the FD is influenced by the rough structural features of the object since all tiles would contain a foreground image.

There is no conclusion on the best algorithm to measure FD of trabecular bone to estimate implant stability. However, power spectrum analysis has its disadvantage in limitation of ROI shape only to a square one. Therefore, ROI placement to match the root form of adjacent teeth is more difficult. [27]

6) Image resolution

Güniz Baksi et al. [49] studied the effect of image resolution on FD calculation, using differential box counting method on digital periapical radiographs of

dry human mandibles. Images obtained with higher resolution scans (651 dpi) gave significantly higher FD values compared to lower resolution scans (397 dpi). This effect was partially due to the fact that increasing resolution results in smaller observable details. Moreover, higher level of noise can be detected as resolution increases. These two factors contribute to the elevation of FD value.

For CBCT, Ibrahim et al. [56] studied the effect of scan parameters on bone microstructural measurement in an edentulous mandibular cadaver. The scan parameters were varied among 5 different fields of view (FOV; 4x4, 6x6, 8x8, 10x10 and 10x5 cm), between 2 rotation acquisition types (180 and 360 degree) and between 2 scanning resolutions (standard and high). Only FOV parameter was found to have significant effect on bone microstructural measurements, especially in small FOV. With a larger FOV, trabecular number increased while trabecular thickness and trabecular spacing decreased. It was suggested that these altered measurements might due to increasing image artefacts from greater amount of structures outside the field which disturbed the reconstruction process. [56, 58] Furthermore, with increased FOV, the voxel size increases as well. As larger voxel has a higher contrast-to-noise ratio (CNR), the visual resolution of the large-voxel images might be better than the small-voxel images. Thus, the higher CNR in larger voxel may also account for the difference in these microstructural measurements and for FD discrepancy among varying FOVs. However, no significant effect from both rotation step and scanning resolution were reported. Therefore, the half rotation and standard resolution are recommended to reduce the patient exposure dose and shorten the reconstruction time. [56]

Pauwels et al. [50] studied FD in bone samples and concluded that FD decreased at larger voxel size (0.160 mm to 0.300 mm). However, in contrast to previous study, they discussed the possible explanation as larger voxel results in lower spatial resolution and loss of trabecular detail. The images become increasingly blurred, and the trabecular structure gradually gets lost as merging of adjacent trabeculae occur. Their results showed continuing increased FD values in smaller voxel sizes that contained higher noise from non-compensated mAs samples. Thus it appears that the noise has a

smaller effect on bone structure analysis than voxel size. This was consistent with previous study [55] which also confirmed the clear effect of the voxel size on observers' scores for image quality, regarding spatial resolution and contrast resolution.

CHAPTER III
RESEARCH METHODOLOGY

Materials and Methods

The study protocol was approved by the Human Research Ethics Committee of the Faculty of Dentistry, Chulalongkorn University, Bangkok, Thailand (HREC-DCU 2017-015).

Patients receiving implant placements at Faculty of Dentistry, Chulalongkorn University, during 2011-2017 were screened for their demographic data (age and sex) and treatment records. The implant sites with maximum 6 months pre-placement CBCT examination and available detailed dental record including IT or ISQ by means of Osstell Mentor instrument (Integration Diagnostics) values were included. Additional details involving implantation sites, implant geometry (shape, thread, cervical microthread and size) were collected. Patients with any underlying diseases or medical condition, affecting bone quality, were excluded from the sample group.

CBCT datasets were obtained from two machines, 3D Accuitomo 170 (J.Morita, USA Inc.) and i-CAT next generation platinum Cone Beam 3D system (Imaging Sciences International, LLC, USA) with a resolution of 0.16, 0.25 and 0.29 mm and exposure parameter of 80-90 kVp, 5-9 mA and 120 kVp, 5 mA, respectively. All CBCT data were exported in DICOM format, and reconstructed using CS 3D Imaging Software (Carestream Dental, USA). Cross-sectional slices were reconstructed by one operator, at 3.8-4.3 mm thickness in the center of each implant site, according to provided gutta percha markers and post-operative radiographs. The images then underwent 4X magnification, and were captured as TIFF files.

Images were then converted into 8-bits gray scale images using Image J software version 1.51 (National Institutes of Health, Bethesda, MD. http://rsb.info.nih.gov/nih-image). Two rectangular regions of interest (ROI) were selected within the same slice. The first ROI was set to cover the highest height of alveolar ridge within the possible path

of insertion (HROI). Another ROI was selected to cover most of the alveolar width (WROI). Root surface of the adjacent teeth and cortical bone were excluded from the ROIs. Area of ROI was recorded in pixel number.

All ROIs were processed according to methods described previously by White and Rudolph [59] as summarized in Figure 27. The tile counting method were applied with a box size ranging from 5-12, 3-7 and 3-6 pixels for 0.16, 0.25 and 0.29 mm-image resolution, respectively. These were adjusted, regarding the optimal range of box size for trabecular bone between 0.132-0.396 mm as described in previous study. [53] A log-log plot of the number of boxes, needed to cover the skeletonized trabecular image, was created against the varying box sizes. FD value was derived from slope of a straight fitted line. Repeated FD measurement was performed in 15 samples at 2 week-interval to assess intra-observer reliability.

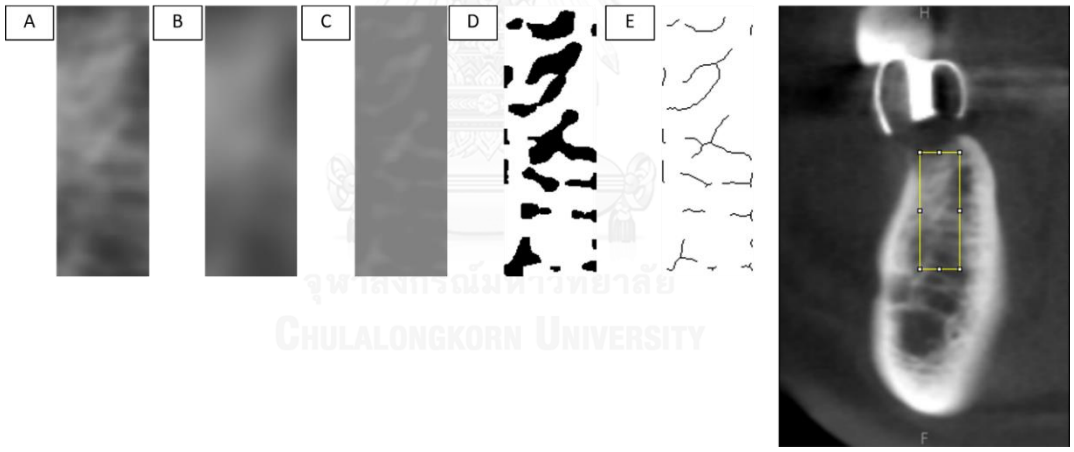

Figure 27. shows the morphological binary image processing prior to FD calculation. A: Region of interest, B: Blurred image, C: Subtracted image (add value of 128), D: Binary image, E: Skeletonized image

Statistical Analysis

Paired t-test was performed between HROI and WROI for FD and mean area differences. Univariate analyses were performed to evaluate the effect of FD and other affecting factors on ISQ and IT. Mann-whitney test were used to investigate the effect of

sex, implantation location, implant shape, implant thread and cervical microthread on ISQ and IT. Spearman's rho test were used to explore the effect of FD, age, implant diameter and implant length on ISQ and IT. All significant affecting factors were further included in subsequent multiple regression analyses to get their adjusted correlation with ISQ or IT. (along with imaging parameter, in case FD was included.) Paired t-test was used to assess intra-observer reliability of FD measurement. Significant level was set at 95% confident interval. SPSS software version 17.0 (SPSS Inc) was utilized.

CHAPTER IV
RESULTS

Part I Comparison between HROI and WROI

Sixty eight pairs of ROI were submitted to paired t-test. No significant difference was found between FD values ($p = 0.779$) but a significant difference was found between area of ROI. ($p < 0.001$) Therefore, area of ROI was not included as confounding factor and HROI was used in further regression analyses, investigating correlation between FD and implant stability.

Paired t-test between repeated FD pairs as intra-observer reliability test revealed no statistically significant difference at $p = 0.881$.

Part II Regarding ISQ

Seventy seven implant sites were included from 21 females and 12 males with mean age of 58.93$\pm$6.50 years (44.27-66.33 years) and 56.18$\pm$11.11 years (38.64-73.55 years), respectively. All implant data are shown in Table 3.

Table 3. Distribution of subjects for each implant parameter regarding ISQ affecting factors

Implant site	Number (N)
Maxilla	27
Mandible	50
Implant shape	**Number (N)**
Cylindrical	49
Tapered	28
Implant thread	**Number (N)**
V-shaped	72
Buttress	5
Cervical microthread	**Number (N)**
With microthread	44
Without microthread	33

Implant size	Diameter (mm)							Total (N)
	3.3	3.6	4.1	4.2	4.5	4.8	5.0	
8	1		3			3		7
9		2		24	4	1	3	34
10	6		10			11		27
11				4	2	1		7
12	1		1					2
Total (N)	8	2	14	28	6	16	3	77

The ISQ values ranged from 17 to 83 (mean 67.78±13.392). Univariate analyses revealed three statistically significant affecting factors on ISQ. Negative effect of maxillary tooth location on ISQ was noted, comparing to mandibular tooth location ($p<0.001$). Implant diameter was detected with significant positive outcome on ISQ ($p=0.004$). Cervical microthread was also shown with significant positive effect on ISQ. ($p=0.022$) Table 4 shows univariate analysis results for each studied factors with possible influences on ISQ.

Table 4. Univariate analysis results for each studied factors with possible influences on ISQ

Mann-Whitney test		
		Asymp. Sig. (2-tailed)
Sex		0.495
Upper/lower location		<0.001*
Cylindrical/Tapered shape		0.112
V-shaped/Buttress thread		0.521
Cervical microthread		0.022*
Spearman's rho test		
	Correlation Coefficient	Sig. (2-tailed)
Age	-0.101	0.382
Implant diameter	0.327	0.004*
Implant length	-0.118	0.307

* Significant effect on dependent variable, ISQ

Only implant sites with implant data and proper CBCT data were included for ISQ-FD relationship analysis. Implant sites with grafted bones or bone reconstruction before CBCT examination and those with unspecified implantation location were excluded. Since implant sites gave significant effect on ISQ, three univariate correlation analyses were performed, one with a pooled data, using both maxillary and mandibular sites and other 2 separated analyses, using maxillary and mandibular group, respectively.

In pooled data, fifty four implant sites were obtained from 18 females and 10 males with mean age of 57.74$\pm$6.89 years (44.27-66.07 years) and 57.78$\pm$10.19 years (38.64-73.17 years), respectively. The ISQ values range from 17 to 83 (mean 68.43$\pm$12.769). The FD values range from 0.6357 to 0.9979 (mean 0.8685$\pm$0.0679).

In maxillary group, sixteen implant sites were obtained from 4 females and 6 males with mean age of 62.27$\pm$4.43 years (52.60-66.07 years) and 53.86$\pm$13.46 years (38.64-73.17 years), respectively. The ISQ values range from 30 to 81 (mean 63.69$\pm$14.131). The FD values range from 0.7769 to 0.9979 (mean 0.8786$\pm$0.0588). All X-ray exposure parameters (resolution and machine) and implant data were shown in Table 5.

Table 5. Distribution of maxillary subjects for each implant data and CBCT parameter in regarding to correlation between FD and ISQ

Implant size	Diameter (mm)						Total (N)
	3.3	4.1	4.2	4.5	4.8	5.0	
8		1					1
9			2	2		3	7
10	2	3			2		7
12		1					1
Total (N)	2	5	2	2	2	3	16
Implant shape							Number (N)
Cylindrical							9
Tapered							7
Implant thread							Number (N)
V-shaped							16
Buttress							-
Cervical microthread							Number (N)
With microthread							7
Without microthread							9
X-ray machine			Resolution (mm)				Total (N)
			0.16	0.25			
3D Accuitomo 170, J.Morita			2	13			15
3D i-CAT next generation platinum			-	1			1
Total (N)			2	14			16

In mandibular group, thirty eight implant sites were obtained from 15 females and 7 males with mean age of 56.23±6.97 years (44.27-65.34 years) and 60.02±7.44 years (45.33-70.87 years), respectively. The ISQ values range from 17 to 83 (mean 70.42±11.781). The FD values range from 0.6357 to 0.9939 (mean 0.8642±0.0716). All X-ray exposure parameters (resolution and machine) and implant data were shown in Table 6.

Table 6. Distribution of mandibular subjects for each implant data and CBCT parameter in regarding to correlation between FD and ISQ

Implant size	Diameter (mm)						Total (N)
	3.3	3.6	4.1	4.2	4.5	4.8	
8						2	2
9		2		16	1	1	20
10	1		3			7	11
11				3	2		5
Total (N)	1	2	3	19	3	10	38
Implant shape							Number (N)
Cylindrical							26
Tapered							12
Implant thread							Number (N)
V-shaped							38
Buttress							-
Cervical microthread							Number (N)
With microthread							27
Without microthread							11
X-ray machine	Resolution (mm)						Total (N)
	0.16		0.25				
3D Accuitomo 170, J.Morita	5		21				26
3D i-CAT next generation platinum	-		12				12
Total (N)	5		33				38

The result revealed no significant correlation between ISQ and FD values in all groups. However, one intriguing finding was the opposite effect of FD on ISQ between maxillary and mandibular group. FD was reported with positive effect (correlation coefficient) in maxillary group while the effect was negative in mandibular group. Table 7 demonstrates univariate analysis results for correlation between ISQ and FD in each group. Scattered plot between ISQ and FD in pooled data was illustrated in Figure 28.

Table 7. Univariate analysis results for correlation between ISQ and FD

Spearman's rho test		
	Correlation Coefficient	Sig. (2-tailed)
Pooled data	-0.099	0.478
Maxillary group	0.111	0.683
Mandibular group	-0.174	0.295

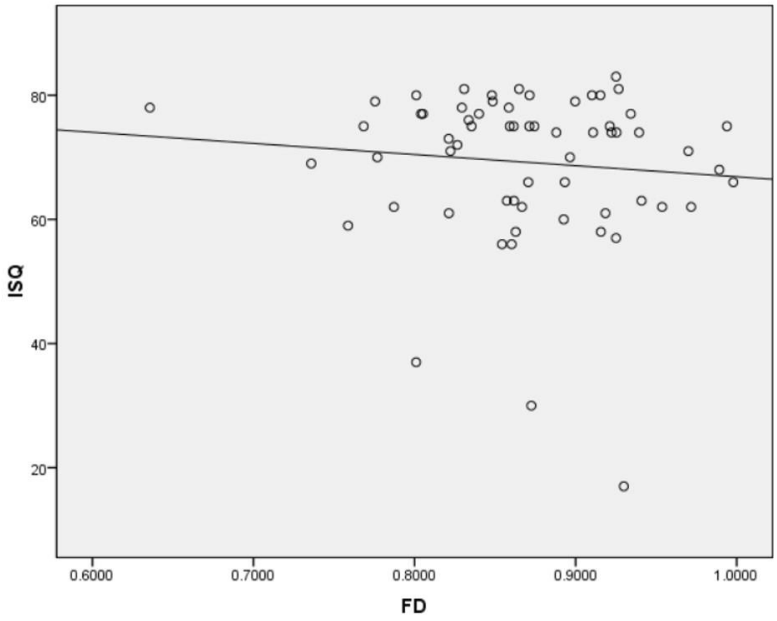

Figure 28. Scatter plot between ISQ and FD values

Therefore, only the 3 statistically significant factors related to ISQ, as shown in previous univariate analyses: implant diameter, implantation location and cervical microthread, were included in multiple linear regression to adjust for age and sex. Seventy four implant sites were included from 20 females and 12 males with mean age of 58.71±6.57 years (44.27-66.33 years) and 55.95±11.20 years (38.64-73.55 years), respectively. All significant implant data were shown in Table 8.

Table 8. Distribution of subjects for multiple linear regression regarding ISQ affecting factors

Implant site	Number (N)
Maxilla	25
Mandible	49
Cervical microthread	**Number (N)**
With microthread	43
Without microthread	31

Implant size	Diameter (mm)							Total (N)
	3.3	3.6	4.1	4.2	4.5	4.8	5.0	
8	1		3			3		7
9		2		24	4		3	33
10	6		9			11		26
11				4	2	1		7
12	1							1
Total (N)	8	2	12	28	6	15	3	74

The ISQ values ranged from 37 to 83 (mean 69.62±9.856). Three outliers were removed from the regression analysis (ISQ value of 17, 20, 30). Multiple linear regression analysis revealed statistically significant negative effect of maxillary tooth location on ISQ, comparing to mandibular tooth location (p=0.005). Implant diameter was also detected with significant positive outcome on ISQ. (p=0.001) Table 9 demonstrates multiple linear regression analysis of all influencing factors on ISQ.

Table 9. Multiple linear regression analysis of all factors affecting ISQ

	Unstandardized Coefficients		Standardized Coefficients	T	Sig.
	B	Std. Error	Beta		
Constant	33.160	12.501		2.653	0.010
Age	0.037	0.119	0.034	0.307	0.759
Sex	3.177	2.103	0.162	1.511	0.135
Maxillary location[a]	-6.491	2.214	-0.314	-2.932	0.005*
Implant diameter	7.783	2.191	0.358	3.552	0.001*
Cervical microthread	3.484	2.425	0.176	1.437	0.155

* Significant effect on dependent variable, ISQ

a: Mandibular location was used as reference.

Part III Regarding IT

Eighty two implant sites were included from 19 females and 13 males with mean age of 60.34±5.52 years (46.48-66.33 years) and 57.56±10.36 years (38.64-73.55 years), respectively. All implant data are shown in Table 10.

Table 10. Distribution of subjects for each implant parameter regarding IT affecting factors

Implant site	Number (N)
Maxilla	33
Mandible	49
Implant shape	**Number (N)**
Cylindrical	57
Tapered	25
Implant thread	**Number (N)**
V-shaped	72
Buttress	10
Cervical microthread	**Number (N)**
With microthread	37
Without microthread	45

Implant size	Diameter (mm)							Total (N)
	3.3	3.6	4.1	4.2	4.5	4.8	5.0	
8	1		4			5		10
9		2		23	3	1	3	32
10	7		16			10		33
11				2		1		3
12	1		2			1		4
Total (N)	9	2	22	25	3	18	3	82

The IT values range from 10 to 45 (mean 29.15±9.552). Univariate analyses revealed no statistically significant affecting factors on IT. Table 11 shows univariate analysis results for each studied factors with possible influences on IT.

Table 11. Univariate analysis results for each studied factors with possible influences on IT

Mann-Whitney test		
		Asymp. Sig. (2-tailed)
Sex		0.713
Upper/lower location		0.243
Cylindrical/Tapered shape		0.510
V-shaped/Buttress thread		0.649
Cervical microthread		0.200
Spearman's rho test		
	Correlation Coefficient	Sig. (2-tailed)
Age	0.016	0.890
Implant diameter	0.141	0.205
Implant length	0.018	0.870

Only implant sites with implant data and proper CBCT data were included for IT-FD relationship analysis. Implant sites with grafted bones or bone reconstruction before CBCT examination and those with unspecified implantation location were excluded. Since opposite effect of FD between maxillary and mandibular group had been shown in part II, three univariate correlation analyses were performed, one with a pooled data, using both maxillary and mandibular sites and other 2 separated analyses, using maxillary and mandibular group, respectively.

In pooled data, fifty two implant sites were obtained from 16 females and 11 males with mean age of 59.68$\pm$6.07 years (46.48-66.21 years) and 58.36$\pm$9.86 years (38.64-73.17 years), respectively. The IT values range from 10 to 45 (mean 30.19$\pm$9.495). The FD values range from 0.7587 to 0.9979 (mean 0.8769$\pm$0.0547).

In maxillary group, eighteen implant sites were obtained from 4 females and 7 males with mean age of 62.27$\pm$4.43 years (52.60-66.07 years) and 55.14$\pm$12.44 years (38.64-73.17 years), respectively. The IT values range from 15 to 45 (mean 30.83$\pm$8.090). The FD values range from 0.7769 to 0.9979 (mean 0.8780$\pm$0.0559). All X-ray exposure parameters (resolution and machine) and implant data were shown in Table 12.

Table 12. Distribution of maxillary subjects for each implant data and CBCT parameter in regarding to correlation between FD and IT

Implant size	Diameter (mm)						Total (N)
	3.3	4.1	4.2	4.5	4.8	5.0	
8		1					1
9			2	2		3	7
10	2	4			2		8
12		1			1		2
Total (N)	2	6	2	2	3	3	18
Implant shape							Number (N)
Cylindrical							11
Tapered							7
Implant thread							Number (N)
V-shaped							18
Buttress							-
Cervical microthread							Number (N)
With microthread							7
Without microthread							11
X-ray machine	Resolution (mm)						Total (N)
	0.16		0.25				
3D Accuitomo 170, J.Morita	2		13				15
3D i-CAT next generation platinum	-		3				3
Total (N)	2		16				18

In mandibular group, thirty four implant sites were obtained from 13 females and 7 males with mean age of 58.60±6.44 years (46.48-66.21 years) and 60.50±7.41 years (45.33-70.87 years), respectively. The IT values range from 10 to 45 (mean 29.85+10.261). The FD values range from 0.7587 to 0.9939 (mean 0.8763±0.0550). All X-ray exposure parameters (resolution and machine) and implant data were shown in Table 13.

Table 13. Distribution of mandibular subjects for each implant data and CBCT parameter in regarding to correlation between FD and IT

Implant size	Diameter (mm)					Total (N)
	3.3	3.6	4.1	4.2	4.8	
8					1	1
9		2		15	1	18
10	2		4		7	13
11				1		1
12			1			1
Total (N)	2	2	5	16	9	34
Implant						Number (N)
Cylindrical						26
Tapered						8
Implant						Number (N)
V-shaped						33
Buttress						1
Cervical microthread						Number (N)
With microthread						20
Without microthread						14
X-ray machine	Resolution (mm)					Total (N)
	0.16		0.25	0.29		
3D Accuitomo 170, J.Morita	4		23	-		27
3D i-CAT next generation	-		6	1		7
Total (N)	4		29	1		34

The result revealed statistically significant negative correlation between IT and FD values only in mandibular groups. Table 14 demonstrates univariate analysis results for correlation between IT and FD in each group. Scattered plot between IT and FD in pooled data, maxillary and mandibular group were illustrated in Figure 29.

Table 14. Univariate analysis results for correlation between IT and FD

Spearman's rho test		
	Correlation Coefficient	Sig. (2-tailed)
Pooled data	-0.263	0.059
Maxillary group	-0.005	0.985
Mandibular group	-0.412	0.016*

* Significant effect on dependent variable, ISQ

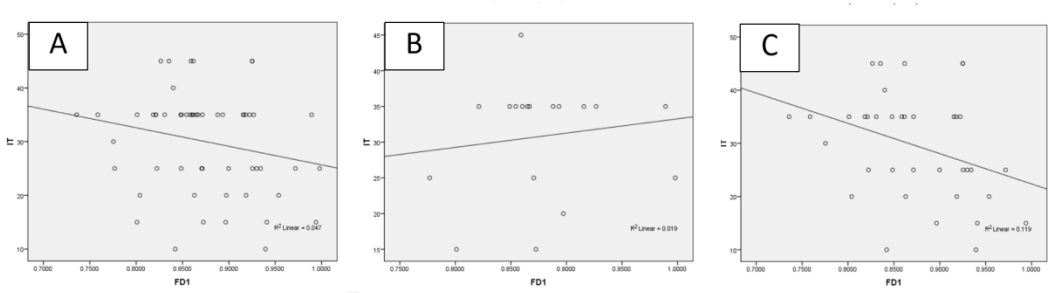

Figure 29. Scattered plot between IT and FD

A. Pooled data

B. Maxillary group

C. Mandibular group

Therefore, only FD and X-ray exposure parameters (resolution and machine) from mandibular group were included in multiple linear regression to adjust for age and sex. Thirty four implant sites were obtained from 13 females and 7 males with mean age of 58.60±6.44 years (46.48-66.21 years) and 60.50±7.41 years (45.33-70.87 years), respectively. All X-ray exposure parameters were shown in Table 13.

The IT values range from 10 to 45 (mean 29.85+10.261). The FD values range from 0.7587 to 0.9939 (mean 0.8763±0.0550). Significant correlation was found between IT, FD and X-ray machine used with a regression model as followed

Model 1: IT = 93.511 - 74.926(FD) (+ 9.708 if 3D i-CAT next generation platinum was used.) (R^2 = 0.295, p = 0.004)

Model 2: IT = 92.168 – 71.112(FD) (R^2 = 0.145, p = 0.026)

Table 15 demonstrates multiple linear regression analysis of influencing factors on a correlation between IT and FD in mandibular group.

Table 15. Multiple linear regression analysis of all factors affecting correlation between IT and FD in mandibular group

		Unstandardized Coefficients		Standardized Coefficients	T	Sig.
		B	Std.	Beta		
Model 1	Constant	93.511	24.715		3.784	0.001
	FD	-74.926	28.183	-0.401	-2.659	0.012
	Machine[a]	9.708	3.774	0.388	2.572	0.015
Model 2	Constant	92.168	26.790		3.440	0.002
	FD	-71.112	30.514	-0.381	-2.331	0.026

a: 3D Accuitomo 170, J.Morita was used as reference

CHAPTER V
DISCUSSION AND CONCLUSION

Discussion

Primary implant stability depends mostly on immediate mechanical engagement between implant and surrounding bone during implantation. [10] Therefore, degree of implant stability can be affected by various factors associating to bone-implant interface, regarding quantity and quality of bone, implant geometry (length, diameter, shape and threads) and surgical technique. [4] Thus, 3 variables, affecting the bone quality, including age, sex and implantation location, were included as possible influencing factors in statistical analyses of ISQ and IT. Other 3 variables, affecting the bone-contact surface of implant, including implant diameter, length and design (shape, thread and microthread), were also included. However, due to a limitation of a retrospective study, surgical technique and data regarding any complication cannot be retrieved. Hence, the drilling dimension and effective length were not studied in the analysis. Nevertheless, all implantations were done in Faculty of Dentistry, Chulalongkorn university. Therefore, a standard protocol, regarding surgical technique, could be assumed.

RFA and IT are commonly used as non-invasive clinical methods to determine implant stability. [5, 10] RFA provide an objective measurement for implant stability with a resonance frequency analyzer and transducer. The analysis is based on structural and vibration principle where a magnetic impulse is generated and transferred onto an implant via an attached transducer. Response signals are then picked up by a receptor vibration to induce an electric voltage in the resonance frequency analyzer. [3, 4, 12] The frequency with the highest amplitude, representing the implant-bone unit's stiffness, is translated to ISQ value of 0 to 100. [5, 10, 27, 28, 30]

IT is a force used to insert an implant into a prepared osteotomy, combining of the thread placement force at implant tip and the friction against the lateral bone as implant enters the site. [60, 61] A peak IT is obtained near the final seating step by the force of

the implant's butt against the bottom bone and the contact of the implant flange with crestal bone, combined with interfacial stress along the implant surface. [20, 27]

According to different concept between RFA and IT, it should be noted that IT represents the whole bone stiffness along the implant length, accounting for the frictional resistance of the bone bed at apical portion and rotating resistant force around its longitudinal axis, while RFA may reveal bone-implant engagement and its resistance to lateral displacement. [62] RFA is presumed to affect mostly in the upper part of the alveolar ridge. [63] Since the transducer is attached on top of the implant, the provided frequency pulse may give more significant effect in the crestal region. Previous study also reported consistent result, where significant correlation between cutting torque and ISQ was only observed at the crestal bony region. [34] Two other studies also stated that there was no overall correlation between IT and ISQ. [61, 64] With these findings, different confounding factors affecting ISQ and IT are expected.

The result revealed a significant positive effect of implant diameter on ISQ. Wider implant diameter has been shown to increases primary stability due to the increased bone–implant contact surface area. [20, 33, 36] In accordance with this study, recent retrospective analysis for effect of multiple factors on ISQ also revealed a positive effect of larger implant diameter on ISQ both at the time of implantation and before restoration when taking into account various factors, that possibly effect ISQ, consisting of sex, age, maxilla/mandibular location, immediate/delayed implantation, presence or absence of bone grafting, implant diameter, implant length, healing pattern, insertion torque and bone type. [3] This gave a stronger model since the coefficient of correlation is weighted among other variables. Another recent multivariate study also yielded similar results which demonstrated significantly higher ISQ with greater implant diameter. [33] Moreover, RFA measures the stability when apply lateral force relevant to clinically bending force. [20, 36] Therefore, amount of circumferential bone surrounding implant, rather than longitudinal bone volume, might play an important role in RFA measurement. Hence, greater effect of implant diameter on ISQ was found, comparing to implant length.

However, no significant correlation was found between implant diameter and IT. This also support an aforementioned speculation that ISQ value implies the bone-implant contact at the crestal margin since implant diameter represents the cervical width of the implant in both cylindrical and tapered shape. Therefore, effect of implant diameter might be more significant on ISQ.

Although longer implant also creates higher bone-implant contact, different implant length was found with no significant change in both ISQ and IT. This is in consistent with previous work, measuring both ISQ and IT, that no effect of implant length on stability is observed. [64] Moreover, since ISQ was found to correlate with bone stiffness (IT) only at the crestal region. [34] Therefore, increasing in implant length might not significantly alter the ISQ value. Furthermore, the positive effect could be minimized since it was suggested that longer drilling time may lead to over preparation of implant site, loosening the implant-bone interface thus decreasing implant stability. [36] Lastly, more number of threads move past the bone in longer implant, these repeated contact could result in bone deformation, leading to reduced stability. [35]

Several implant designs have been released to improve implant stability with modifications in number, orientation and spacing of thread (thread pitch). Greater number of thread and smaller pitch results in larger functional surface area which increase resistance to applied force. [65] However, due to limited information on thread pitch, this factor was excluded from the study. Nevertheless, this effect was speculated via the presence of cervical microthread which gave a positive effect on ISQ in an univariate analysis. Larger sample size may be required to reveal its significant effect in multiple linear regression. Recent study also found similar result with greater stability in implant with cervical microthread, compared with cylindrical implant. [33] No significant correlation was detected between cervical microthread and IT. This again encourages a hypothesis that ISQ demonstrates the bone-implant contact at the crestal margin thus more significant effect of cervical microthread is observed.

Thread geometry is another factor, influencing implant stability. Study of reverse torque and bone-implant contact (BIC) of 3 different implant threads, placed in rabbit tibia,

reported significantly more BIC and greater reverse-torque from square threaded-implants, comparing to the V-shaped and reverse buttress thread designs which gave a similar results. [66] This is in consistent with present study since no significant difference in effect on IT and ISQ was found between implant with buttress thread and V-shaped thread.

Another adaptation is in the implant shape where tapered implants are developed to create a lateral compression to the bone during insertion thus increasing the bone-implant interface stability. [20, 33, 67] However, controversial results arose when investigating effect of implant shape on both ISQ and IT. Tapered implant showed no significant difference in implant stability, comparing to cylindrical one. This was in accordance with previous study which stated that significant torque increases from a certain value (34 Ncm) did not largely decrease micromotion. [62] Thus, tapered implant, that gives higher torque, might result in comparable ISQ values to cylindrical one with other improved design. Moreover, this finding may be explained by the effect of the drilling dimension which was not included in the analysis, due to incomplete data on surgical procedure. As small drill size can affect the local compression thus IT can be increased, even in cylindrical implants. [41] Furthermore, these modified geometries may result in over-compression in good bone quality. [20] Commonly, significantly higher IT was needed to insert a tapered implant. However, there is a maximum limit to this compression where implant cannot be inserted further, resulting in an un-seated implant which require an re-insertion with a larger drill size. The problem remain as the taper end of the implant might not engage the apical portion of the bone. [20, 68] Therefore, IT might be decreased despite the use of tapered implant. Recent multivariate study also found lesser effect of taper implant when taking other confounding variables of implant location, platform, gender and bone quality into account. [36]

Nevertheless, when analyzing effect on ISQ, all these additional designs seem to be out-shadowed by the effect of bone quality. Implantation location has been shown in several studies to affect ISQ. Maxillary implants often have lower ISQ than mandibular implants. [3, 33, 64] Previous study also reported that most implants in maxilla had ISQ

< 60 while mandibular implants often had ISQ $\geq$ 60. [31] As bone quality plays an important role in primary stability, it also gives possible explanations to this finding as well. It was suggested that maxillary bone is often softer due to less cortex. [36] Another study also reported a mean bone mineral density of the mandible at 1.11 g/cm^2, which is much larger than that in the anterior maxilla (mean = 0.55 g/cm^2) or the posterior maxilla (mean = 0.31 g.cm^2). [69] The bone density from computed tomography also demonstrates similar trend where 846±234 HU, 526±107 HU, 591±176 HU, 403±95 HU were recorded in the anterior mandible, posterior mandible, anterior maxilla, and posterior maxilla respectively, with a significant correlation between bone density and ISQ value. [70] In contrast to ISQ, IT was insignificantly affected by different jaw position. This may be explained by the engagement of implant thread to cortical bone on bucco-lingual aspect of alveolar ridge. This additional cortical entrapment might lead to greater IT in low bone quality, as previous study in rabbit revealed higher removal torque with more cortical bone in implant thread. [71] Consistently, study of Akkocaoglu, et al. also demonstrated high IT values where apical fixation of implant to cortical bone occurred, regardless of relatively low ISQ. [63]

The word “fractal” has been used to describe an entity with self-similarity, a property in which a magnified subset is indistinguishable from the whole object. [42-44] The concept of fractal analysis (FA) arises in order to quantify these complexities. [43] Radiographic bone trabecular architecture could be analyzed, usually with tile counting method since cancellous bone has been shown to possess self-similarity property and magnification-dependent metric property. [5, 43-45] For CBCT, kVp was concluded to have no significant influence on FD at constant radiation dose. [50] Therefore, this parameter was excluded from our analysis. Greater resolution is more capable in detecting fine bone structure. With lesser resolution, the images are blurred, and trabeculae become merging to adjacent bone, leading to significantly lower FD. [49, 50, 52] Differences in image quality were shown between various CBCT machines, resulting from difference in spatial resolution, contrast resolution, noise, and geometric accuracy.

[55] This inconsistency in image quality might also affect FD calculation. Thus, resolution and X-ray machine were included in the model analysis as influencing factors to FD.

According to statistical analysis in mean area difference from 2 types of ROI, a significant difference was detected. Thus the comparison between two FD values from different ROI types was performed. No significant difference in FD was found. Therefore, it was feasible to concluded that area of the ROI plays no significant role in FD calculation. Further investigation of FD from CBCT images were conducted with no attempt to restrict the size of the ROI. This finding is consistent with previous work by Shrout et al. [46] who reported no significant effect on FD when non-standardized ROIs were used.

Our study found no significant correlation between ISQ and FD. One explanation is that ISQ values represent the bone–implant contact rather at the marginal bone region than at deeper parts. [63] However, FD values were measured along the alveolar height in present study hence a correlation might be hard to obtained. This result was in contrast with previous studies which had detected a significant correlation between ISQ and FD from pre-operative panoramic radiographs. [5, 28] This could also be contributed to less image resolution (0.25 mm), used in most of our samples. Since larger FOV were needed in order to cover all implantation sites in one scan, the voxel size increased. As resolution decreases, fine bone structure becomes blurred and merge to each other. [52] Hence, less difference in bone complexity among different bone quality could be detected. Therefore, with this resolution, differences in FD among each samples might not be large enough to differentiate various bone quality for ISQ. Furthermore, CBCT grey values are affected by the partial volume effect (PVE). [56] The voxels that contain both bone and marrow information will have an ambiguous grey value, resulting in difficulty in classifying them as foreground or background. With large voxel sizes, the influence of PVE can result in thicker trabeculae or loss of thin trabeculae which might also lead to the FD alteration. [57] Therefore, further prospective multivariate study with higher image resolution is needed to establish a conclusive result in correlation between ISQ and FD.

From the analysis of possible affecting factors on ISQ in pooled samples, it was speculated that implantation location plays an important role in determining ISQ values.

Therefore, in order to investigate the effects of other variables, the samples were then divided into two study groups; maxillary and mandibular tooth location. Although significant correlation between ISQ and FD was not found in both maxillary and mandibular group, one intriguing finding was that FD was reported with positive effect (correlation coefficient) in maxillary group while the effect was negative in mandibular group. Possible explanation is the difference in trabecular structure between maxilla and mandible found in this study group. Maxillary trabeculae tend to be finer and grainy thus, with more trabecular number, the complexity increases, so does the FD value. In mandible, bone trabeculae tend to be coarser and thicker, similar to a linear structure. Hence, the denser the trabeculae, the more linear with less grain it become, leading to less complexity detected, so does the FD values. (Figure 30)

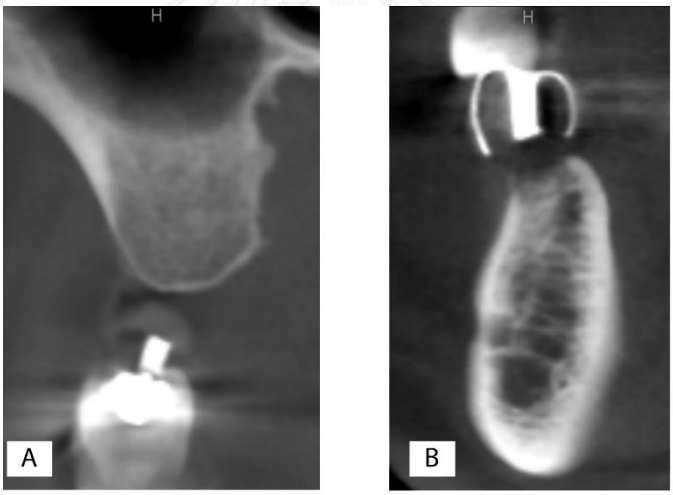

Figure 30. Difference in trabecular pattern between maxillary (A) and mandibular (B) sample with the same ISQ (value = 81) but different FD (A=0.9267 and B=0.8308)

When investigating correlation between IT and FD value in pooled data, no significant correlation was found. However, from the aforementioned speculation in ISQ analysis, an attempt was made to testify the different trend of FD, observed in maxillary and mandibular samples. Thus the pooled data was classified in 2 groups of different jaw types. FD was reported with the same trend, negative effect in mandibular group. With

both findings in IT and ISQ analysis, it was proposed that the implant stability prediction, using FD, should be separate into maxillary and mandibular group. Further study with larger sample size is needed to test this hypothesis as well.

A significant correlation was found between IT, FD and X-ray machine used. This was in consistent with previous finding that different CBCT devices gave a wide range of image quality, resulting from difference in spatial resolution, contrast resolution, noise, and geometric accuracy. [55] Thus, alteration in FD, among different X-ray machine, could be expected. Therefore, both models were accepted with the model equations:

Model 1: IT = 93.511 - 74.926(FD) (+ 9.708 if 3D i-CAT next generation platinum was used.) (R^2 = 0.295, p = 0.004)

Model 2: IT = 92.168 – 71.112(FD) (R^2 = 0.145, p = 0.026)

Model 1 is preferable when FD was obtained, using CBCT data from either 3D i-CAT next generation platinum or 3D Accuitomo 170. Model 2 is proposed as an equation where other CBCT devices were used. However, the R^2 value of 0.145 means that the model can explain only 14.5 percent of the variability of IT. This is relatively low and may not give clinically significant prediction of IT. Previous studies by Tolga Suer, B., et al. [5] and Veltri et al. [27] report a correlation between IT and FD with higher R^2 value of 0.2045 and 0.447, respectively. However, these two studies were well-controlled and evaluated the pure correlation of IT and FD without any confounding variables. When taking multiple variables from the clinical level into account, a decrease in the ability of the model to predict IT was foreseeable.

According to present study, FD seems to have more significant effect on IT rather than ISQ. This is in consistent with previous work by Veltri et al. [27] who reported only correlation between IT and FD of 16 implants in rabbit femurs. (R^2=0.447) The possible explanation might due to the fact that IT represents the bone stiffness along the implant length, while RFA may reveal bone-implant engagement mostly on the crestal region. [34, 62] As the ROI, used for FD, covers not only the crestal part but the length of the alveolar ridge with in possible path of insertion, FD value is likely to be more correlated with IT.

Conclusions

1) Different ROIs; maximizing bone height VS maximizing bone width, does not affect FD calculation in CBCT.
2) ISQ values at implant placement were significantly affected by implant diameter and implantation jaw sites. However, no significant correlation was found between ISQ and FD in both maxillary and mandibular groups.
3) IT values significantly correlate with FD in mandibular group.

REFERENCES

1. John, V., Chen, S., and Parashos, P. Implant or the natural tooth—a contemporary treatment planning dilemma? Australian dental journal 52 (2007): S138-S150.
2. Tyndall, D. A., et al. Position statement of the American Academy of Oral and Maxillofacial Radiology on selection criteria for the use of radiology in dental implantology with emphasis on cone beam computed tomography. Oral surgery, oral medicine, oral pathology and oral radiology 113 (2012): 817-826.
3. Huang, H., Wismeijer, D., Shao, X., and Wu, G. Mathematical evaluation of the influence of multiple factors on implant stability quotient values in clinical practice: a retrospective study. Therapeutics and clinical risk management 12 (2016): 1525-1532.
4. Sennerby, L. and Meredith, N. Implant stability measurements using resonance frequency analysis: biological and biomechanical aspects and clinical implications. Periodontology 2000 47 (2008): 51-66.
5. Tolga Suer, B., Yaman, Z., and Buyuksarac, B. Correlation of Fractal Dimension Values with Implant Insertion Torque and Resonance Frequency Values at Implant Recipient Sites. International Journal of Oral & Maxillofacial Implants 31 (2016): 55-62.
6. Meredith, N. Assessment of implant stability as a prognostic determinant. International Journal of Prosthodontics 11 (1998): 491-501.
7. Brunski, J. B. Biomechanical factors affecting the bone-dental implant interface. Clinical materials 10 (1992): 153-201.
8. Sennerby, L. The implant stability quotient whitebook: The relationship between reliable diagnostics and safe, successful dental implant procedures.[Online]. Available from: http://www.osstell.com/wp-content/uploads/2015/03/25045-00-EN-ISQ-Whitebook.pdf[2017, July 18]

9. Swami, V., Vijayaraghavan, V., and Swami, V. Current trends to measure implant stability. The Journal of the Indian Prosthodontic Society 16 (2016): 124-130.

10. Atsumi, M., Park, S. H., and Wang, H. L. Methods used to assess implant stability: current status. International Journal of Oral & Maxillofacial Implants 22 (2007): 743-754.

11. Saurabh, G. and Rubina, K. Implant stability measure: Critical review of various methods. Dent Implants Dentures 1 (2016): 100-110.

12. Mistry, G., Shetty, O., Shetty, S., and Singh, R. D. Measuring implant stability: A review of different methods. Journal of Dental Implants 4 (2014): 165-169.

13. Sullivan, D. Y., Sherwood, R. L., Collins, T. A., and Krogh, P. H. The reverse-torque test: a clinical report. International Journal of Oral & Maxillofacial Implants 11 (1996): 179-185.

14. Ivanoff, C. J., Sennerby, L., and Lekholm, U. Reintegration of mobilized titanium implants: An experimental study in rabbit tibia. International journal of oral and maxillofacial surgery 26 (1997): 310-315.

15. Wyatt, C. C. and Pharoah, M. J. Imaging techniques and image interpretation for dental implant treatment. International Journal of Prosthodontics 11 (1998): 442-452.

16. Misch, C. Dental Implant Prosthetics. St. Louis: Elsevier Mosby, 2005.

17. Teerlinck, J., Quirynen, M., Darius, P., and van Steenberghe, D. Periotest⇔: An Objective Clinical Diagnosis of Bone Apposition Toward Implants. International Journal of Oral & Maxillofacial Implants 6 (1991): 55-61.

18. Goswami, M., Kumar, M., Vats, A., and Bansal, A. Evaluation of dental implant insertion torque using a manual ratchet. Medical journal armed forces india 71 (2015): S327-S332.

19. Raghavendra, S., Wood, M. C., and Taylor, T. D. Early wound healing around endosseous implants: a review of the literature. International Journal of Oral & Maxillofacial Implants 20 (2005): 425-431.

20. Meredith, N. A review of implant design, geometry and placement. Appl Osseointgrated Res 6 (2008): 6-12.

21. Szmukler-Moncler, S., Piattelli, A., Favero, G. A., and Dubruille, J. H. Considerations preliminary to the application of early and immediate loading protocols in dental implantology. Clinical oral implants research 11 (2000): 12-25.

22. Meredith, N., Books, K., Fribergs, B., Jemt, T., and Sennerby, L. Resonance frequency measurements of implant stability in viva. A cross-sectional and longitudinal study of resonance frequency measurements on implants in the edentulous and partially dentate maxilla. Clinical oral implants research 8 (1997): 226-233.

23. Meredith, N., Shagaldi, F., Alleyne, D., Sennerby, L., and Cawley, P. The application of resonance frequency measurements to study the stability of titanium implants during healing in the rabbit tibia. Clinical oral implants research 8 (1997): 234-243.

24. Heo, S., et al. Stability measurements of craniofacial implants by means of resonance frequency analysis. A clinical pilot study. The Journal of Laryngology & Otology 112 (1998): 537-542.

25. Balleri, P., Cozzolino, A., Ghelli, L., Momicchioli, G., and Varriale, A. Stability measurements of osseointegrated implants using Osstell in partially edentulous jaws after 1 year of loading: a pilot study. Clinical implant dentistry and related research 4 (2002): 128-132.

26. Moy, P. The ISQ scale in daily practice: Cut-off values for different indications [Online]. 2014. Available from: http://www.osstell.com/videos-lectures/the-benefits-of-resonance-frequency-analysis-rfa/[2017, July 18]

27. Veltri, M., Ferrari, M., and Balleri, P. Correlation of radiographic fractal analysis with implant insertion torque in a rabbit trabecular bone model. International Journal of Oral & Maxillofacial Implants 26 (2011): 108-114.

28. Lee, D. H., et al. A clinical study of alveolar bone quality using the fractal dimension and the implant stability quotient. Journal of periodontal & implant science 40 (2010): 19-24.

29. Andreotti, A. M., et al. Relationship Between Implant Stability Measurements Obtained by Two Different Devices: A Systematic Review. Journal of periodontology 88 (2017): 281-288.

30. Pattijn, V., et al. Resonance frequency analysis of implants in the guinea pig model: influence of boundary conditions and orientation of the transducer. Medical engineering & physics 29 (2007): 182-190.

31. Nedir, R., Bischof, M., Szmukler-Moncler, S., Bernard, J. P., and Samson, J. Predicting osseointegration by means of implant primary stability. Clinical oral implants research 15 (2004): 520-528.

32. Tözüm, T. F., Dursun, E., and Uysal, S. Radiographic fractal and clinical resonance frequency analyses of posterior mandibular dental implants: their possible association with mandibular cortical index with 12-month follow-up. Implant dentistry 25 (2016): 789-795.

33. Gehrke, S. A., et al. Stability of implants placed in fresh sockets versus healed alveolar sites: early findings. Clinical oral implants research 27 (2016): 577-582.

34. Friberg, B., Sennerby, L., Meredith, N., and Lekholm, U. A comparison between cutting torque and resonance frequency measurements of maxillary implants: A 20-month clinical study. International journal of oral and maxillofacial surgery 28 (1999): 297-303.

35. Kheur, M. G., Sandhu, R., Kheur, S., Le, B., and Lakha, T. Reliability of resonance frequency analysis as an indicator of implant micromotion: an in vitro study. Implant dentistry 25 (2016): 783-788.

36. Östman, P. O., Hellman, M., Wendelhag, I., and Sennerby, L. Resonance frequency analysis measurements of implants at placement surgery. International Journal of Prosthodontics 19 (2006): 77–83.

37. Barikani, H., et al. The effect of implant length and diameter on the primary stability in different bone types. Journal of dentistry (Tehran, Iran) 10 (2013): 449-455.

38. Alsaadi, G., Quirynen, M., Michiels, K., Jacobs, R., and Van Steenberghe, D. A biomechanical assessment of the relation between the oral implant stability at insertion and subjective bone quality assessment. Journal of clinical periodontology 34 (2007): 359-366.

39. Checa, S. and Prendergast, P. J. Effect of cell seeding and mechanical loading on vascularization and tissue formation inside a scaffold: a mechano-biological model using a lattice approach to simulate cell activity. Journal of biomechanics 43 (2010): 961-968.

40. Burger, E. H. and Klein-Nulend, J. Mechanotransduction in bone—role of the lacuno-canalicular network. The FASEB Journal 13 (1999): S101-S112.

41. Campos, F. E., et al. Effect of drilling dimension on implant placement torque and early osseointegration stages: an experimental study in dogs. Journal of Oral and Maxillofacial Surgery 70 (2012): e43-e50.

42. Geraets, W. and Van der Stelt, P. Fractal properties of bone. Dentomaxillofacial Radiology 29 (2000): 144-153.

43. Lopes, R. and Betrouni, N. Fractal and multifractal analysis: a review. Medical image analysis 13 (2009): 634-649.

44. Sánchez, I. and Uzcátegui, G. Fractals in dentistry. Journal of dentistry 39 (2011): 273-292.

45. Benhamou, C., et al. Fractal organization of trabecular bone images on calcaneus radiographs. Journal of bone and mineral research 9 (1994): 1909-1918.

46. Shrout, M. K., Potter, B. J., and Hildebolt, C. F. The effect of image variations on fractal dimension calculations. Oral Surgery, Oral Medicine, Oral Pathology, Oral Radiology, and Endodontology 84 (1997): 96-100.

47. Jolley, L., Majumdar, S., and Kapila, S. Technical factors in fractal analysis of periapical radiographs. Dentomaxillofacial Radiology 35 (2006): 393-397.

48. Ruttimann, U. E., Webber, R. L., and Hazelrig, J. B. Fractal dimension from radiographs of peridental alveolar bone: a possible diagnostic indicator of osteoporosis. Oral surgery, oral medicine, oral pathology 74 (1992): 98-110.

49. Baksi, B. G. and Fidler, A. Image resolution and exposure time of digital radiographs affects fractal dimension of periapical bone. Clinical oral investigations 16 (2012): 1507-1510.

50. Pauwels, R., Faruangsaeng, T., Charoenkarn, T., Ngonphloy, N., and Panmekiate, S. Effect of exposure parameters and voxel size on bone structure analysis in CBCT. Dentomaxillofacial Radiology 44 (2015): 20150078.

51. Shrout, M., Hildebolt, C., and Potter, B. The effect of varying the region of interest on calculations of fractal index. Dentomaxillofacial Radiology 26 (1997): 295-298.

52. Bollen, A., Taguchi, A., Hujoel, P., and Hollender, L. Fractal dimension on dental radiographs. Dentomaxillofacial Radiology 30 (2001): 270-275.

53. Huh, K. H., et al. Fractal analysis of mandibular trabecular bone: optimal tile sizes for the tile counting method. Imaging science in dentistry 41 (2011): 71-78.

54. Oshida, Y., Hashem, A., Nishihara, T., and Yapchulay, M. Fractal dimension analysis of mandibular bones: toward a morphological compatibility of implants. Bio-medical materials and engineering 4 (1994): 397-407.

55. Pauwels, R., et al. Comparison of spatial and contrast resolution for cone-beam computed tomography scanners. Oral surgery, oral medicine, oral pathology and oral radiology 114 (2012): 127-135.

56. Ibrahim, N., et al. The effect of scan parameters on cone beam CT trabecular bone microstructural measurements of the human mandible. Dentomaxillofacial Radiology 42 (2013): 20130206.

57. Kothari, M., et al. Impact of spatial resolution on the prediction of trabecular architecture parameters. Bone 22 (1998): 437-443.

58. Araki, K. and Okano, T. The effect of surrounding conditions on pixel value of cone beam computed tomography. Clinical oral implants research 24 (2013): 862-865.

59. White, S. C. and Rudolph, D. J. Alterations of the trabecular pattern of the jaws in patients with osteoporosis. Oral Surgery, Oral Medicine, Oral Pathology, Oral Radiology, and Endodontology 88 (1999): 628-635.

60. Johansson, P. Assessment of bone quality from cutting resistance during implant surgery. Int J Oral Maxillofac Implants 9 (1994): 279-288.

61. da Cunha, H. A., Francischone, C. E., Fliho, H. N., and de Oliveira, R. C. G. A comparison between cutting torque and resonance frequency in the assessment of primary stability and final torque capacity of standard and TiUnite single-tooth implants under immediate loading. International Journal of Oral & Maxillofacial Implants 19 (2004): 578-585.

62. Brizuela-Velasco, A., et al. Relationship between insertion torque and resonance frequency measurements, performed by resonance frequency analysis, in micromobility of dental implants: an in vitro study. Implant dentistry 24 (2015): 607-611.

63. Akkocaoglu, M., Uysal, S., Tekdemir, I., Akca, K., and Cehreli, M. C. Implant design and intraosseous stability of immediately placed implants: a human cadaver study. Clinical oral implants research 16 (2005): 202-209.

64. Fuster-Torres, M. Á., Peñarrocha-Diago, M., Peñarrocha-Oltra, D., and Peñarrocha-Diago, M. Relationships between bone density values from cone beam computed tomography, maximum insertion torque, and resonance frequency analysis at implant placement: a pilot study. International Journal of Oral & Maxillofacial Implants 26 (2011): 1051–1056.

65. Misch, C. E., et al. Rationale for the application of immediate load in implant dentistry: part II. Implant dentistry 13 (2004): 310-321.

66. Steigenga, J., Al-Shammari, K., Misch, C., Nociti Jr, F. H., and Wang, H. L. Effects of implant thread geometry on percentage of osseointegration and resistance to reverse torque in the tibia of rabbits. Journal of periodontology 75 (2004): 1233-1241.

67. Glauser, R., et al. Resonance frequency analysis of implants subjected to immediate or early functional occlusal loading. Clinical oral implants research 15 (2004): 428-434.

68. O'sullivan, D., Sennerby, L., and Meredith, N. Influence of implant taper on the primary and secondary stability of osseointegrated titanium implants. Clinical oral implants research 15 (2004): 474-480.

69. Devlin, H., Horner, K., and Ledgerton, D. A comparison of maxillary and mandibular bone mineral densities. The Journal of prosthetic dentistry 79 (1998): 323-327.

70. Turkyilmaz, I. and McGlumphy, E. A. Influence of bone density on implant stability parameters and implant success: a retrospective clinical study. BMC Oral Health 8 (2008):

71. Sennerby, L., Thomsen, P., and Ericson, L. E. A morphometric and biomechanic comparison of titanium implants inserted in rabbit cortical and cancellous bone. International Journal of Oral & Maxillofacial Implants 7 (1992): 62–71.

VITA

Miss Napassorn Kangvansurakit was born on 27th July 1987. She graduated her Doctor of Dental Surgery from Chulalongkorn University in 2012. After graduation, she worked at Sirindhorn College of Public Health Suphanburi as a general practitioner and lecturer for 2 years. After that, she became a lecturer in Faculty of Dentistry, Western University. In 2015, she started her Master degree at Chulalongkorn University in Department of Radiology and continued ever since.